

Opsin-based photoreception in Crinoids

Youri Nonclercq¹, Marjorie Lienard², Alexia Lourtie¹, Emilie Duthoo¹, Lise Vanespen¹, Igor Eeckhaut¹, Patrick Flammang¹, Jérôme Delroisse^{1,3*}

¹ Laboratory of Biology of Marine Organisms and Biomimetics, Research Institute for Biosciences, University of Mons, Belgium

² Laboratory of Molecular Biology of Sensory Systems, GIGA, University of Liège, Belgium

³ Laboratory of Cellular and Molecular Immunology, GIGA, University of Liège, Belgium

* **Corresponding author:** jerome.delroisse@umons.ac.be; youri.nonclercq@umons.ac.be

E-mail addresses : marjorie.lienard@uliege.be; igor.eeckhaut@umons.ac.be; patrick.flammang@umons.ac.be; alexia.lourtie@umons.ac.be; emilie.duthoo@umons.ac.be; lise.vanespen@student.umons.ac.be

Abstract

Opsin-mediated light perception has been investigated in many marine invertebrates including some clades of echinoderms such as sea stars, sea urchins and brittle stars. On the other hand, the understanding of potential light perception in crinoids, the basal lineage of the echinoderm phylum, remains largely unexplored. Only a few behavioural observations suggest that crinoids may be sensitive to light stimuli.

This study investigates the behavioural and molecular basis of opsin-based photoreception in *Antedon bifida*, a European crinoid species belonging to the Comatulid order. In this context, the behavioural response to different light wavelengths, the characterisation of opsin genes in the recent chromosome-scale genome of this species and the opsin immunolocalisation within the crinoid tissues have been investigated.

Behavioural tests pointed to a significant negative phototactic behaviour induced by a wide range of light wavelengths (463 to 630 nm) with maximum sensitivity to blue light ($\lambda_{max} = 463$ nm). *In silico* genome analyses revealed the presence of only three rhabdomeric opsin genes located on chromosomes 4 and 6: *Abif-opsins 4.1*, *4.2* and *4.3*. All crinoid opsins are phylogenetically clustered as a sister-group of all other echinoderm rhabdomeric opsins, supporting their evolution via duplication of an ancestral gene in the crinoid lineage. The low opsin diversity contrasts with other echinoderms which are generally characterised by up to eight bilaterian opsin groups. Interestingly, *A. bifida* opsin sequences present typical amino acid residues of rhabdomeric opsins of other bilaterians, including two conserved cysteines (C110, C187), the probable ancestral E181 counterion, a NPxxY(x)₆F pattern, a highly conserved lysine potentially covalently bound to a chromophore, and the (D)RY motif, all supportive of photoreceptive functions. Finally, immunoreactivity to newly generated antibodies designed against sea star opsins was highlighted in several tissues associated with the ambulacral grooves of the calyx and the pinnules. Within these tissues, *Abif-opsins* (potentially the *Abif-opsin 4.1*) are expressed in the ectoneural basiepithelial nerve plexus-and the hyponeural nerve plexus. On the other hand, a different opsin type (potentially the *Abif-opsin 4.2*) is also expressed in the sensory papillae of tube feet. The localization of at least two opsin types in different sensory structures suggests the presence of a complex extraocular photoreception system exclusively based on rhabdomeric opsins in this crinoid species.

Keywords

Crinoidea – Opsin – Photoreception – Echinodermata – Negative phototaxis

46 Background

47

48 Light plays a major role in marine ecosystems. Most marine organisms have specific photosensitive
49 organs, such as eyes, which contain opsins, the prototypic light-sensitive GPCR receptors of
50 eumetazoans. Interestingly, echinoderm often lack specialised visual organs with the exception of
51 optic cushions located at the tip of sea star arms [Takasu and Yoshida 1983; Johnsen 1997; Garm and
52 Nilsson 2014; Petie et al. 2016] and putative eyespots in a few holothurian species [Berrill 1966,
53 Yamamoto and Yoshida 1978]. However, numerous ethological observations confirm that most
54 investigated echinoderms are light-sensitive [for review, Yoshida et al. 1984, Sumner-Rooney and
55 Ullrich-Lüter 2023]. Most echinoderm species are then characterised by extraocular photoreception
56 abilities, mediated by different classes of opsins expressed in different tissues, organs and structures
57 intimately connected to the nervous system. Two types of opsins, ciliary and rhabdomeric, have been
58 particularly investigated and identified in various adult anatomical structures, such as tube feet,
59 integument, and spines of sea urchins [Ullrich-Lüter et al. 2011; 2013], sea stars [Delroisse et al. 2013,
60 Ullrich-Lüter et al. 2013, Clarke et al. 2024] and brittle stars [Moore and Cobb, 1985; Cobb and Hendler,
61 1990; Delroisse et al. 2014; 2016; Sumner-Rooney et al. 2018; 2020; 2021]. In addition, sea stars
62 (Asteroidea), the optic cushion is specifically expressing several opsin types [Ullrich-Lüter et al. 2011,
63 Lowe et al. 2018]. A third type of opsin, a GO-opsin, has also been identified in two clusters of sensory
64 cells on either side of the apical organ of pluteus sea urchin larvae [Valero-Gracia et al. 2016; Valencia
65 et al. 2021; Cocurullo et al. 2023]. Extensive phylogenetic analyses of bilaterian opsins have shown that
66 echinoderms are one of the phyla that have the largest diversity of ancestral opsin types with 7 opsin
67 classes on a total of 9 predicted in the common ancestor of all bilaterians [D'Aniello et al. 2015; Ramirez
68 et al. 2016]. Some of these ancestral opsin types, like bathyopsins and chaopsins, are currently almost
69 exclusively restricted to echinoderms [Ramirez et al. 2016].

70 The crinoid group has been the least studied echinoderm class in terms of sensory perception
71 in general, and photoreception in particular. However, given that Crinoidea currently represents the
72 most basal clade of echinoderms, separated from the other orders since at least the Lower Ordovician
73 period *i.e.* 480 million years ago, their phylogenetic position makes them an interesting group to better
74 understand the evolution of photoreception not only within the whole phylum. It has long been known
75 that some crinoid species are sensitive to light stimuli. Indeed, ethological observations have shown
76 that several species of comatulid (an order of crinoids, most of which are non-pedunculated in the
77 adult stage) living at shallow depths are predominantly nocturnal, extending their arms to filter feed
78 at night [Magnus 1964, Rutman and Fishelson 1969, Meyer 1973, Vail 1987]. On the other hand, when
79 these organisms are exposed to daylight, they tend to hide in reef crevices or under shaded
80 underwater overhangs. Other observations point to rapid retraction of their arms when exposed to
81 strong sunlight [Meyer 1973]. This nocturnal activity is however less and less systematically observed
82 in individuals living at greater depths (beyond 10-20 m below the surface) where the luminosity of the
83 environment is lower [Fishelson 1974]. Some studies have also reported a swimming escape behaviour
84 in these feather stars, such as the European species *Antedon bifida*, when exposed to strong light
85 stimuli [Dimelow 1958]. However, these isolated observations leave many unexplored areas, such as
86 a deeper characterisation of the photoreceptive behaviours, or a determination of the spectral
87 sensitivity of these animals. No photosensitive sensory structure has yet been formally demonstrated
88 in extant crinoids. The repertoire of opsin genes also remains mostly unexplored, with only one
89 rhabdomeric-type opsin so far identified in two transcriptome datasets from *Antedon mediterranea*
90 and *Florometra serratissima* [D'Aniello et al. 2015].

91 The highly specialised lifestyle of crinoids and their phylogenetic position make them a prime
92 group to better understand the evolution of the large opsin diversity in echinoderms, as well as the
93 evolution of their extraocular photoreception.

94 This study sheds light on the mechanisms of crinoid opsin-based photoreception by focusing
95 on the phototactic behaviour of a model feather star species: *Antedon bifida*. This small common
96 species lives in shallow water, from a few centimetres below the surface down to a depth of 200 m
97 along the North Atlantic European coasts and is generally found during the day in shaded rocky
98 environments, sheltered from full light. Leveraging a recently available chromosome-scale genome,
99 we further annotate and describe the complete opsin gene repertoire in this crinoid species and assess
100 the precise anatomical location of several opsin-based photoreceptors. Altogether our combined
101 behavioural, *in silico*, morphological and expression approaches reveal novel types of candidate
102 photosensitive tissues, opening for molecular and functional studies in this under-studied class of
103 echinoderms.

104

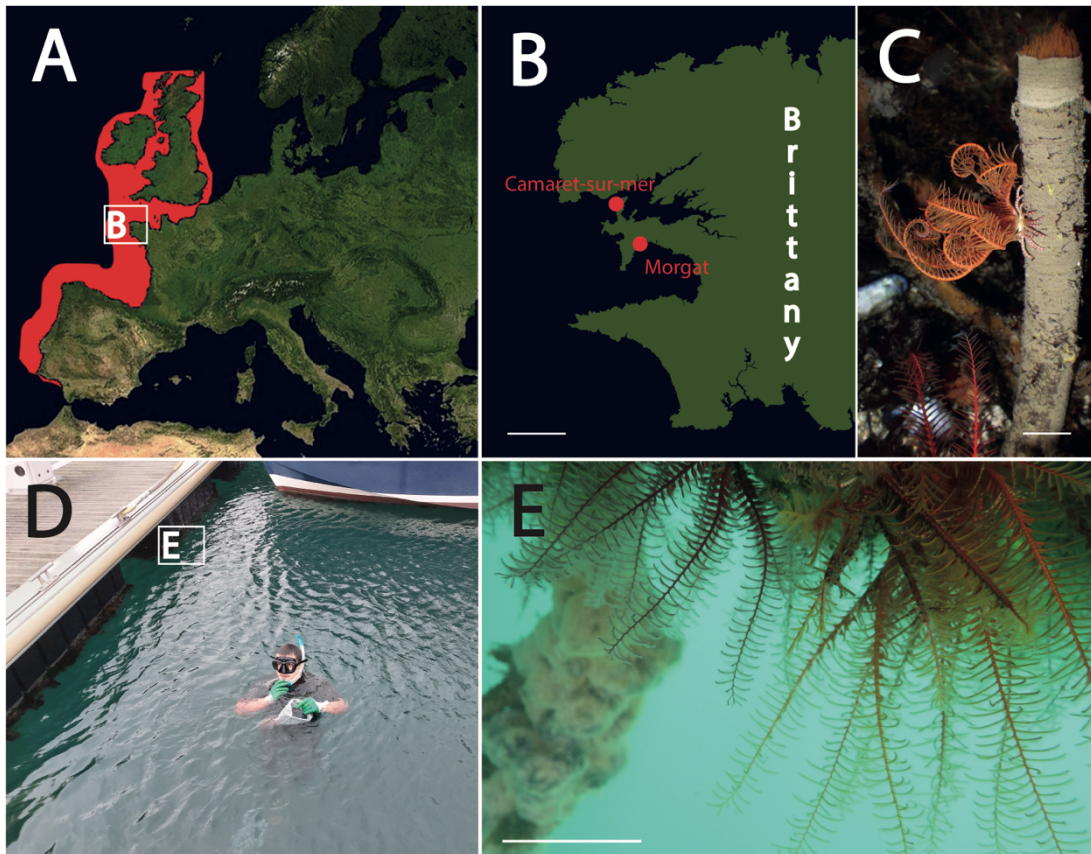
105 Material and Methods

106

107 **Collection of crinoid specimens**

108 Specimens of *Antedon bifida* (**Fig 1 A**) were collected from two coastal harbours on the Crozon
109 peninsula in Brittany, France (**Fig 1B-D**). The organisms were present in large amounts clinging to the
110 underside of boat mooring pontoons, just a few centimetres below the surface (**Fig 1E, F**). Around
111 thirty individuals were brought back to the University of Mons (Belgium) and kept in an aquarium
112 containing around 400 L of seawater at 15°C (with a salinity of 34 PSU) in a closed circuit following a
113 12H/12H day/night cycle (**Fig 1G**).

114



115

116 **Figure 1.** Distribution, habitat, and collection site of *Antedon bifida*. (A) Geographical distribution of *A.*
117 *bifida* on the North Atlantic coasts of Europe. (B) Focus on the two collection sites (Morgat and
118 Camaret-sur-Mer) located on the Crozon peninsula in Brittany (France). (C) Adult specimen of *Antedon*
119 *bifida* clinging to a sabellid tubeworm. (D) Collecting site in the marina of Camaret-sur-mer. (E) The
120 dense population of *A. bifida* hanging under the mooring pontoons. Scales: B. 15km, C. 20mm, E.
121 20mm.

122

123 **Ethological experiments in *Antedon bifida***

124 Phototactic behaviour tests were carried out using a small elongated experimental aquarium (50 cm
125 long and 7.5 cm wide) with three of its sides rendered opaque by black paper (**Fig 2**). A monochromatic
126 light source (LED bulb GU10 of 1 Watt) was placed against the still transparent glass end of the
127 experimental device, creating a light gradient across the entire aquarium. The light intensity along this
128 gradient was measured with a light metre (Digital Lux Meter AR823⁺, Smart Sensor) and the brightness
129 values varied from 46,000 Lux (6.7 $\mu\text{W}/\text{cm}^2$) next the light source to 3,600 Lux (0.5 $\mu\text{W}/\text{cm}^2$) at the
130 opposite extremity. The mean value in the middle part of the aquarium was 10,000 Lux (1.5 $\mu\text{W}/\text{cm}^2$).
131 The floor was covered with a rigid plastic mesh, allowing the crinoids to cling on and easily move in the
132 aquarium. Three different light wavelengths were tested corresponding to blue ($\lambda_{\text{max}}= 463$ nm, half
133 peak bandwidth HBW= 27 nm), green ($\lambda_{\text{max}}= 512$ nm, HBW= 33 nm) and red light ($\lambda_{\text{max}}= 630$ nm, HBW=
134 20 nm). The spectra of each LED lamp were precisely measured beforehand using a spectrometer
135 (Ocean view, FLAM-S-UV-VIS spectrometer). One test was also carried out with polychromatic white
136 light, and a negative control was used without a light source. Each of these five experimental conditions
137 was carried out on 10 individuals of *A. bifida* during the same time of the day in a room completely
138 immersed in darkness. Individuals were tested separately to avoid an aggregation phenomenon. Each
139 crinoid specimen was first conditioned to darkness for around 5 minutes. Then, for each test, each
140 individual was placed in the centre of the aquarium (25 cm from the illuminated end) and its
141 displacement towards (positive displacement) or against (negative displacement) the light source was
142 measured after 10 minutes. These displacement measurements were based on the position of the
143 crinoid calyx centre relative to its initial position. First, statistical tests were used to confirm the
144 homogeneity variance and the normal distribution of the displacement data with Bartlett and
145 Quantil/Quantil tests, respectively. The mean values of the distance covered for each light wavelength
146 tested were then compared to the mean distance travelled by individuals without illumination
147 (negative control), using a one-way analysis of variance (ANOVA), followed by a Dunnett post hoc test
148 with RStudio statistical software.

149

150 ***In silico* identification of opsin genes in crinoids**

151 The diversity of opsin genes in our model crinoid species, *A. bifida*, was determined through a
152 homology-based approach. This method used several published opsin reference sequences as
153 templates [D'Aniello et al. 2015, Ramirez et al. 2016], *i.e.* opsins from the model echinoderm species,
154 the sea urchin *Strongylocentrotus purpuratus*, as well as opsins from additional representative
155 bilaterians (**Suppl. Table S1**).

156 Homology "tBLASTn" searches of predicted protein sequences were performed against the
157 assembled *A. bifida* reference genome (ecAntBifi1.1) available on the NCBI database. The following
158 tBLASTn parameters were used: *Matrix: Blosum62; gap costs: existence 11, extension 1*. We then
159 applied a cut-off e-value $< 10^{-5}$ for putative opsin candidates showing a strong similarity to two highly
160 conserved regions in functional opsins: the 7th transmembrane helix corresponding to the Schiff base
161 binding zone of retinal (equivalent K296 lysine residue in the bovine rhodopsin), and the G-protein
162 binding zone. Since the genome of *A. bifida* has not yet been annotated, a reciprocal BLAST of these

163 selected sequences was then performed on the entire NCBI database to validate their opsin
164 identification.

165 To obtain the most complete and accurate opsin gene predictions, we used several gene
166 prediction softwares like GENSCAN [Burge and Karlin 1997: <http://hollywood.mit.edu/GENSCAN.html>], AUGUSTUS [Oliver et al. 2011: [https://bioinf.uni-](https://bioinf.uni-greifswald.de/augustus/)
167 [greifswald.de/augustus/](https://bioinf.uni-greifswald.de/augustus/)] and FGENESH [Solovyev et al. 2006:
168 <http://www.softberry.com/berry.phtml?topic=index&group=programs&subgroup=gfind>] using
169 tBLASTn on all chromosome portions of the *A. bifida* genome identified to contain opsin loci.

170 Then, we carried out a manual curation as follows: for each predicted opsin, only the longest
171 portion of the protein sequence which, using a MAFFT alignment (MAFFT version 7, Research Institute
172 for Microbial Diseases, Japan, <https://mafft.cbrc.jp/alignment/server/index.html>) [Katoh et al. 2019]
173 and maximising the high similarity to other echinoderm opsin reference sequences (**Suppl. Table S1**)
174 has been selected as the most accurate crinoid opsin sequence.

175 Next, a sequence similarity comparison between opsin sequences found in *Antedon bifida* and
176 the reference opsin repertoire of the sea urchin *S. purpuratus* (Sp-opsin 1; 2; 3.1; 3.2; 4; 5; 6; 7 and 8)
177 was performed using SIAS webtool (Sequence Identity And Similarity, Universidad Complutense de
178 Madrid) (<http://imed.med.ucm.es/Tools/sias.html>).

179 The chromosomal locations of *A. bifida* opsin genes within the genome and the number of
180 intron/exon regions were finally determined using internal tBLASTn search of the candidate protein
181 sequences identified above against the *A. bifida* genome. Gene positions within chromosomes were
182 visualised using IGV (Integrative Genomics Viewer) genome browser [Robinson et al 2023]. The
183 number and position of introns and exons were annotated by combining tBlastn, FGENESH in Softberry
184 [<http://www.softberry.com>], and the Kablammo software [Wintersinger and Wasmuth 2014,
185 <https://kablammo.wasmuthlab.org>].

186 A similar procedure was carried out to determine all opsin sequences of two additional crinoid
187 species: *Anneissia japonica* (Comatulidae) and *Nesometra sesokonis* (Antedonidae like *A. bifida*),
188 whose reference genomes are also present in the NCBI genomic database (ASM1163010v1 and
189 ASM2563120v1, respectively).

190

191 **Phylogenetic analyses of crinoid opsins**

192 A phylogenetic analysis was carried out on opsin protein sequences previously discovered in the two
193 crinoid model species (*A. bifida*, *N. sesokonis*) to highlight their relationship with other opsins. For this
194 analysis, 111 different protein sequences from 21 species representing the 5 echinoderm classes were
195 used alongside opsin sequences of a few other representative groups of bilaterians. These sequences
196 were selected based on public metadata [Delroisse et al. 2014; D'Aniello et al. 2015; Ramirez et al.
197 2016; Lowe et al. 2018] and genomic databases such as NCBI to represent all nine ancestral opsin
198 lineages present in bilaterians (ciliary opsin, bathyopsin, Go-opsin, canonical and non-canonical
199 Rhabdomeric opsin, chaopsin, peropsin/RGR opsin, neuropsin and xenopsin) (**Suppl. Table S1**). Eight
200 additional melatonin receptor protein sequences were added as outgroups. The sequences were then
201 aligned using MAFFT version 7 [Katoh et al. 2019]. The alignment was then trimmed using the TrimAl
202 software tool hosted on the NGPhylogeny.fr online platform
203 (<https://ngphylogeny.fr/tools/tool/284/form>). The tree was constructed using IQ-Tree
204 (<http://iqtree.cibiv.univie.ac.at/>) [Nguyen et al. 2015] based on maximum likelihood analysis with 1000
205 ultrafast bootstraps. The best-fit model recommended by ModelFinder [Kalyaanamoorthy et al. 2017]
206 to our unpartitioned dataset was LG+F+I+G4, and the number of parsimony informative sites was 726
207 on the 1583 amino-acid sites used in total. Tree visualisation was finally performed on the iTOL
208 Interactive Tree Of Life platform (<https://itol.embl.de/>).

209

210

211 **Histology**

212 *Specimen preparation*

213 *Antedon bifida* specimens intended for histological and immunohistochemical analysis were
214 anaesthetised with a 3.5% magnesium chloride in sea water solution for 2 min before being placed 4
215 h in a non-acetic Bouin fixative fluid (75% of a picric acid saturated solution and 25% of formaldehyde
216 commercial solution at 37%). After fixation, samples were decalcified for 2 days with a solution of 2%
217 ascorbic acid and 0.3 M sodium chloride. After complete decalcification, samples were dehydrated for
218 24 h in graded ethanol 70° to 95° followed by a bath of butanol for 24 h at 60°C and finally embedded
219 in paraffin (Paraplast Plus). Five µm-thick sections of arm and calyx samples were cut with a Microm
220 HM340 E microtome and mounted on silane-coated glass slides.

221

222 *Staining and imaging*

223 Transverse sections of the calyx and longitudinal sections of the pinnules were stained with
224 Masson's trichrome stain. Images were taken using a microscope (Orthoplan optical microscope, Leica)
225 equipped with a high sensibility camera (DFT7000 T, Leica) using the Application Suite X software (LAS
226 X, Leica).

227

228 **Immunodetection of opsins on crinoid tissue sections**

229 To detect opsins within the tissues of *A. bifida*, both immunofluorescence and immunohistochemical
230 methods were carried out using two sets of purified polyclonal antibodies. These two primary
231 antibodies, anti-Arub_ops1.1 and anti-Arub_ops4, produced in rabbits by Eurogentec, are directed
232 respectively against ciliary opsin 1.1 (residues 159 to 174) and the c-terminal part of rhabdomeric opsin
233 4 (residues 447 to 461) (**Suppl. Fig. S2**) from the common European sea star species *Asterias rubens*.
234 Histological paraffin sections of the calyx and pinnules of *A. bifida* specimens were used for opsin
235 immunodetection.

236

237 *Immunofluorescence*

238 The dewaxed and rehydrated sample sections were rinsed with a solution of phosphate-
239 buffered saline containing 0.5% Tween (PBS-T) and blocked 1h in PBS-T with 3% BSA (Bovine Serum
240 Albumin). Samples were then incubated overnight at 4°C with either primary anti-opsin 1 antibodies
241 or anti-opsin 4 antibodies at 1:200 dilution. Tissues were then rinsed in PBS-T and incubated 1h with
242 commercial secondary antibodies (goat anti-rabbit IgG coupled to a Texas-Red fluorochrome; Alexa-
243 fluorTM 594, Invitrogen A11012) at 1:100 dilution, revealing red fluorescence (peak at 618 nm) after
244 exposure to an optimum excitation length of 590nm. After a final rinse with PBS-T, the slides were
245 mounted with an aqueous mounting medium (Vectashield, Vector Laboratories) containing DAPI (4',6-
246 diamidino-2-phenylindole) highlighting cell nuclei with blue fluorescence (450-490 nm). Opsin labelling
247 was visualised by an Olympus FV1000D inverted confocal laser scanning microscope under three
248 channels of fluorescence by laser excitation (peak excitation/emission): DAPI (358/461 nm), FITC
249 (495/521 nm) and Texas Red (590/618 nm).

250

251 *Immunohistochemistry*

252 Sections used for immunohistochemistry were treated slightly differently from those used for
253 immunofluorescence. After dewaxing and rehydration, slides were heated in a citrate buffer (0.01 M,
254 pH 6.2) in the microwave (2X5 min, 900 W) to unmask specific antigenic epitopes present in the tissue.
255 Tissues were then immersed in 0.06% hydrogen peroxide to quench endogenous peroxidases. The
256 following steps of rinsing, blocking and incubation treatments with primary antibodies were similar to
257 those described above for immunofluorescence. After a second rinse, the tissues were incubated 1 h
258 with a horse anti-rabbit/peroxidase secondary antibody complex (ImmPressTM Reagent kit, Vector

259 Laboratories). For opsin revelation, sections were incubated 1 to 3 minutes with a PBS-buffered
260 solution (pH 7.2) containing 4 mg/ml DAB (4-dimethylaminoazobenzene) and 0.02% H₂O₂. The sections
261 were counterstained with hemalun/Luxol Blue to enhance the contrast with the brown DAB-
262 immunostaining.

263

264 *Controls*

265 Various negative and positive controls were conducted. Negative controls included omitting
266 the primary antibody or using a pre-immune rabbit serum diluted at 1:2000 in place of the primary
267 antibody. In each case, all control sections were not labelled (**Suppl. Fig. S3**). Sections from tissues of
268 *Asterias rubens*, including the optic cushions, tube feet and nervous system were used as positive
269 controls for the detection of opsins 1 and 4. In all cases, the immunostaining gave the expected results
270 as described in previous publications [Ullrich-Lüter et al. 2011, Clarke et al. 2024].

271

272 **Scanning electron microscopy**

273 Two crinoid specimens were prepared (calyx and arms separated) for precise anatomical observation
274 under a scanning electron microscope. After fixation with non-acetic Bouin's fluid, the specimens were
275 first progressively dehydrated with ethanol before being dried in a chamber using the CO₂ critical point
276 drying technique. The samples were then coated with a thin film of gold and palladium using a Jeol
277 JFC-1100E sputter coater (JEOL Company, Tokyo, Japan). Observations of the fine structure of the
278 pinnules and calyx of the feather star were carried out with a Jeol JSM-7200F scanning electron
279 microscope.

280

281 **Results**

282

283 ***Antedon bifida* is negatively phototactic with a maximum response under blue light.**

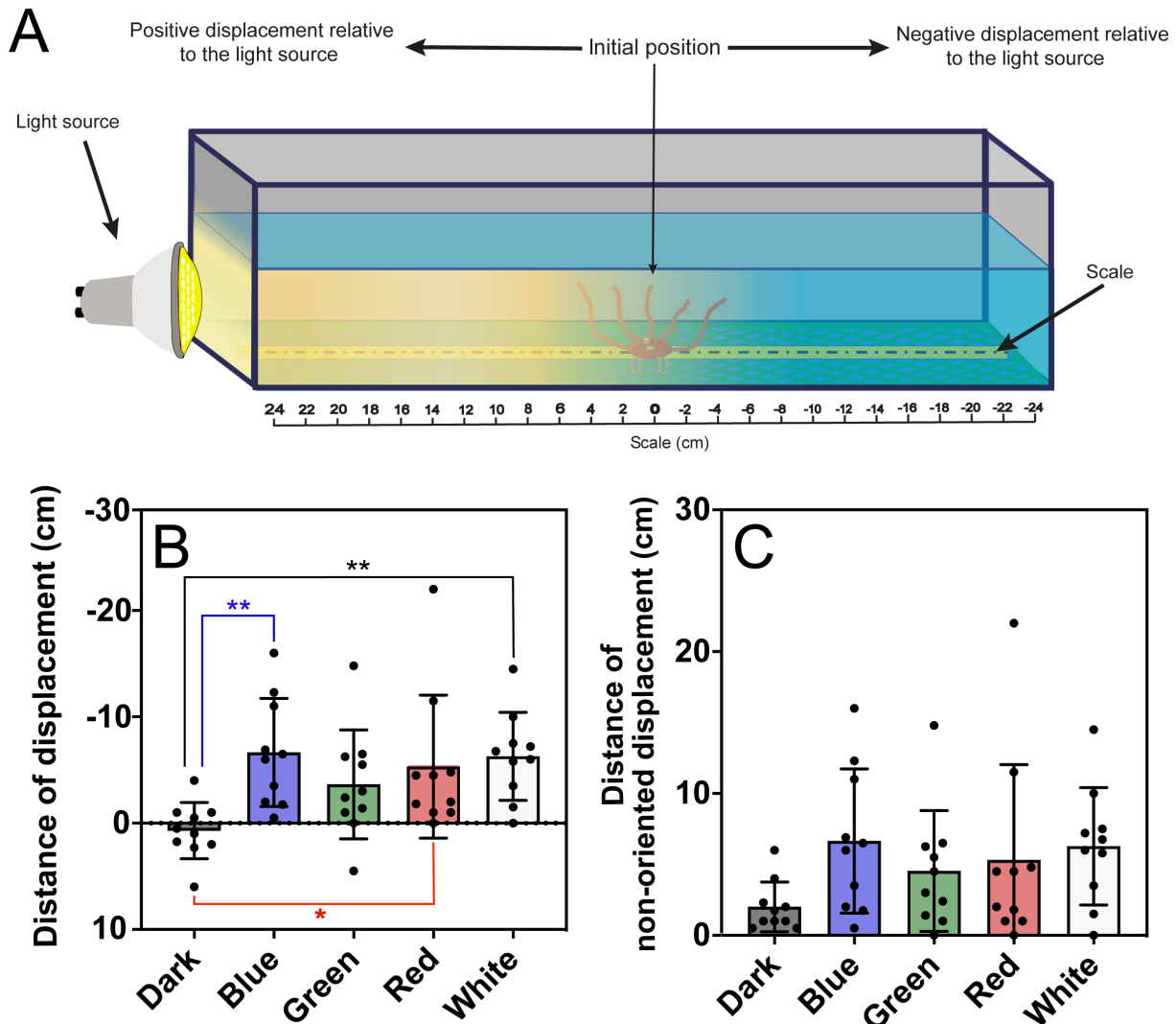
284 Behavioural phototactic tests showed that adult crinoids of the species *A. bifida* were sensitive to white
285 light and moved significantly away from the light source (negatively oriented displacement) compared
286 to the control test without light ($p = 0.0099^{**}$) (**Fig. 2B**). This negative phototactic behaviour was also
287 significant with the red-light ($p = 0.031^{*}$) and reached its maximum amplitude with blue light ($p =$
288 0.0062^{**}). This result points to a high sensitivity of crinoids to the blue part of the visible spectrum. In
289 contrast, the results for the green-light tests showed no significant difference in displacement values
290 compared to the dark control values (green: $p = 0.167$).

291 Displacement values were also normalised by individual calyx size (distance travelled/calyx
292 diameter) to avoid any bias in displacement speed due to variation in individual size. However, we
293 found that there was no correlation between the size of the individuals and the travelled distance
294 during the test. After normalisation, significant differences were only observed for the blue and white
295 lights compared to the dark control.

296 Absolute displacement values were also considered (non-oriented displacements) to
297 determine the reactivity of crinoid individuals to light without considering the direction taken (**Fig. 2C**).
298 As illustrated in Figure 2C, the distances travelled during the test, independently of the direction, did
299 not vary significantly between individuals exposed to the different wavelengths and the controls
300 remaining in the dark.

301 Thus, although light stimuli did not induce significant changes in the mobility of *A. bifida* (non-
302 directional displacement), white, red (630 nm) and blue (463 nm) light stimuli induced a significant
303 directional displacement of crinoids away from the light source (negative phototactic behaviour).

304



305
 306 **Figure 2.** Phototactic behaviour in *Antedon bifida*: (A) Schematic representation of the experimental
 307 aquarium with a light gradient. (B) Graph showing the distance travelled by individuals within the
 308 experimental set-up over 10 minutes of time following different light stimuli (Black = no light; Blue =
 309 λ_{max} of 463 nm; Green = λ_{max} of 512 nm; Red = λ_{max} of 630 nm and White = polychromatic white
 310 light). Negative displacement indicated a displacement away from the light source. One-factor ANOVA
 311 and Dunnett's post hoc statistical tests showed that crinoids exhibited a significant oriented
 312 displacement towards the darker region of the light gradient for white, blue and red light compared
 313 with the no-light control. (C) Graph showing the distances covered by the individuals in absolute
 314 values, showing the rate of movements of crinoids depending on the type of light stimulus. Dunnett's
 315 one-factor ANOVA and post hoc tests did not provide significant results between no-light controls
 316 versus different wavelengths tested.

317

318 ***Antedon bifida* has a reduced opsin repertoire composed of only three rhabdomeric opsins**

319 The homology-based opsin search in the *A. bifida* genome enabled the discovery of three opsin genes:
 320 the *Abif-opsin 4.1* gene present on chromosome 4 [NCBI reference: OY727096.1], the *Abif-opsin 4.2*
 321 and *Abif-opsin 4.3* genes present on chromosome 6 [NCBI reference: OY727098.1] (**Fig. 3B**). The three
 322 predicted *A. bifida* opsins contain, respectively 417, 356 and 408 amino acids (46.42, 41.17 and 45.63
 323 kDa). A clue as to the identification of these three sequences was obtained through reciprocal blast
 324 searches and comparison of the sequence similarity with the set of reference opsins present in the sea




325 urchin *S. purpuratus* and three other non-echinoderm opsin types (**Fig. 3A**). The results showed that
326 the three *A. bifida* opsin sequences have higher similarity with the (non-canonical) rhabdomeric opsins
327 of echinoderms (opsin 4). The same analyses carried out on the genome of another closely related
328 crinoid species, *Nesometra sesokonis*, also revealed the presence of three similar opsin sequences,
329 which also appeared to belong to the rhabdomeric opsin group. On the other hand, research carried
330 out on the genome of the species *Anneissia japonica* (Comatulidae) revealed no opsin genes. It
331 therefore seems that only one bilateral opsin lineage is still present in *A. bifida* and presumably in all
332 Crinoids of the family Antedonidae.

333 All *Abif-opsin* genes share a conserved gene structure composed of one or two short exon
334 sequences (80-270 bp) followed by a third, much longer, terminal exon region (800-960 bp) (**Fig. 3C**).
335 In addition, our genomic analysis of *A. bifida* opsin genes revealed two major structural differences
336 compared to rhabdomeric opsin genes in other echinoderm classes, which lead to an overall shorter
337 gene length due to a lower number of intronic regions (between 1 or 2 introns for *A. bifida* versus 3
338 for sea stars and sea urchins) and reduced intron sizes (between 540 and 1,800 bp maximum for crinoid
339 opsins and from minimum 2,300 bp for the sea star *A. rubens* to maximum 11,400 bp for the sea urchin
340 *S. purpuratus*). Genomic sequence alignments showed homology at the level of the first and last long
341 exon for the three crinoid opsins, as well as for those of sea star and sea urchins. Finally, in the sea star
342 *A. rubens* and the sea urchin *S. purpuratus* opsin 4 orthologs, the regions homologous to the third and
343 fourth exon are fused into a single last exon in the three crinoid opsin sequences. Sequence homology
344 analysis also shows that the first exon of *A. bifida* opsin 4.2 is composed of the assembly of the two
345 first exons homologous to those present in the other two crinoid opsins. A short region of 57 base pairs
346 is also found between these exons, and whose exonic nature recognised by gene prediction software
347 is still uncertain.

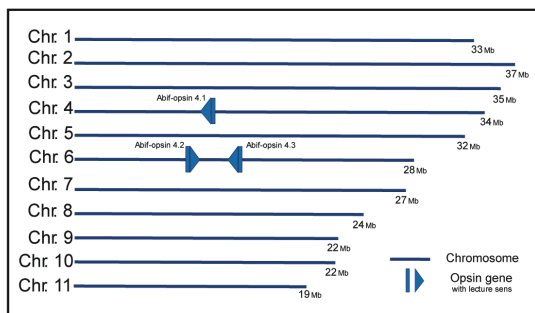
348 Multiple alignment of the predicted opsins found in *A. bifida* and *Nesometra sesokonis* with
349 other rhabdomeric opsins reveals the presence of highly conserved amino acid residues characteristic
350 of light-sensitive opsins (**Fig. 3D**). These opsin characteristics are mainly amino-acids present in the
351 third and seventh transmembrane helix (Tm) as well as in the second extracellular loop (EC), which
352 allow interactions with the conjugated chromophore molecule (retinal) and the G-protein. The most
353 representative opsin residue is a lysine residue in the 7th Tm, corresponding to K296 position in the rat
354 rhodopsin, which performs the Schiff-based covalent binding with the retinal [Terakita 2005]. This
355 lysine is conserved in all aligned predicted opsins of crinoids. For the stabilisation of this protonated
356 Schiff-based binding, a counterion is necessary and this function is typically assumed by a glutamate
357 residue [Terakita et al. 2004; Varma et al. 2019]. The probable ancestral position of this counterion is
358 the equivalent of the glutamate E181 in the rat rhodopsin present in the second extracellular loop.
359 This E₁₈₁, as the only counterion function, is typical of bistable opsins such as rhabdomeric opsins
360 [Terakita et al. 2012; 2014]. The monostable opsins like vertebrate ciliary opsins possess another
361 glutamate counterion in Tm III (corresponding to the E113 in the rat rhodopsin) closer to the retinal
362 binding. This glutamate E₁₁₃ is replaced by a tyrosine residue in rhabdomeric opsins. The three crinoid
363 opsins present the same ancestral counterion glutamate E181, with the tyrosine residue also replacing
364 E113 like in other echinoderm rhabdomeric opsins. These results point to the probable bistable
365 character of crinoid opsins. Another typical amino acid pattern of all GPCR proteins like opsins is the
366 NPxxY(x)₆F pattern (corresponding to the sequence NP_{II}(Y)306 in the rat rhodopsin) which could
367 contribute, amongst other functions, to the binding between the opsin and the G-protein [Fritze et al.
368 2003]. This motif is also present in all the sequences including the Melatonin GPCR receptor. Another
369 tripeptide also seems to participate in the association between the opsin and the G-protein, this is the
370 (D)RY motif (corresponding to the ER(Y)136 in the rat rhodopsin). We can also mention the two opsin-
371 typical cysteine residues (corresponding to C110 in the Tm III and the C187 in the EC II of rat rhodopsin)
372 which allow the stabilisation of protein conformation owing to the formation of a disulfide bridge. The

373 three crinoid opsins possess all these key residues typical of functional opsins. We can also note the
 374 presence, in two of the three crinoid opsins (4.1 and 4.3), of the HxK pattern inside the motif
 375 NPxxY(x)6F, which is rather typical of rhabdomeric opsins and is homologous of the pattern NxQ found
 376 in ciliary opsins (corresponding to the sequence Nx(Q)312 in the rat rhodopsin) [Upton et al. 2021].
 377 This typical-rhabdomeric pattern is only partly present in the crinoid-opsins 4.2 in which the histidine
 378 residue is replaced by a tyrosine. It is interesting to note that this is the only case in the echinoderm
 379 rhabdomeric opsins identified thus far.
 380

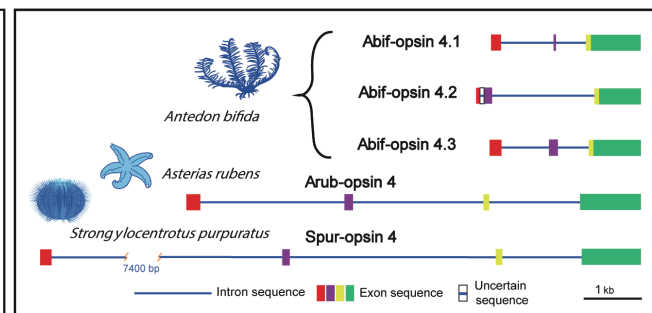
A

	 <i>Rattus norvegicus</i>	 <i>Strongylocentrotus purpuratus</i>										 <i>Lingula anatina</i>
Opsins	Opsin 1 Rhodopsin	Opsin 4 Melanopsin	Opsin 1 Ciliary opsin	Opsin 2 Bathypsin	Opsin 3.1 GO-opsin	Opsin 3.2 GO-opsin	Opsin 4 Rhabdomeric opsin	Opsin 5 Chaopsin	Opsin 6 Peropsin	Opsin 7 R3Rhopsin	Opsin 8 Neuroopsin	Opsin 9 Metopsin
Abif-opsin 4.1	40.22%	41.13%	31.28%	28.04%	30.20%	28.91%	45.53%	37.19%	35.83%	34.27%	28.46%	34.98%
Abif-opsin 4.2	38.32%	46.68%	38.04%	38.61%	36.88%	37.75%	53.31%	36.02%	34.68%	36.74%	36.59%	34.58%
Abif-opsin 4.3	39.36%	46.32%	37.99%	38.23%	37.74%	37.74%	52.45%	37.73%	36.12%	35.68%	36.51%	38.01%

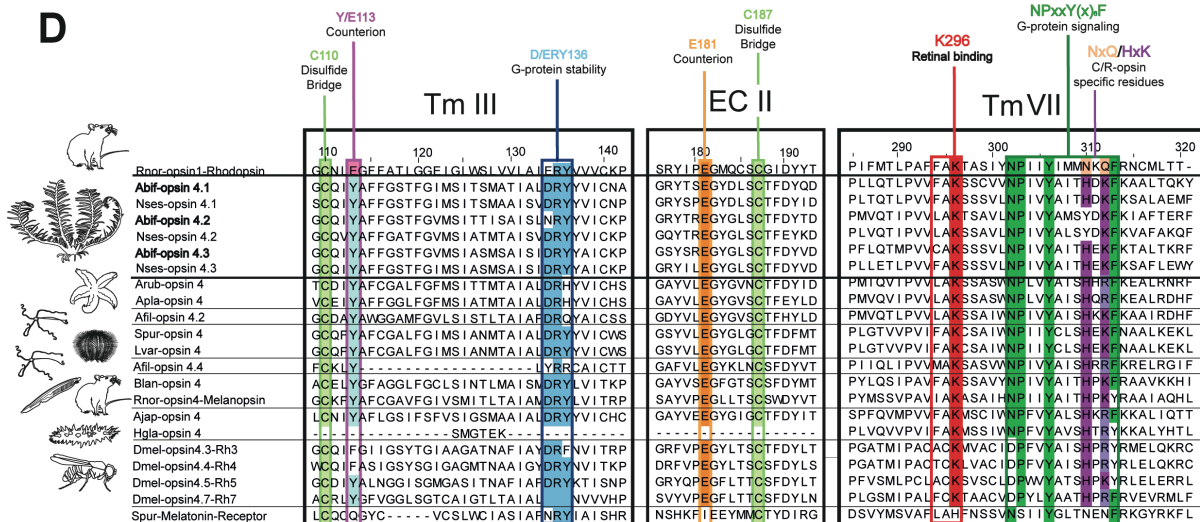
B



C



D



381
 382 **Figure 3.** *In silico* analysis of crinoid opsins: (A) Similarity comparison (%) between the three crinoid
 383 opsin protein sequences predicted from the *Antedon bifida* genome with all echinoderm opsin groups
 384 present in the model species of sea urchin (*Strongylocentrotus purpuratus*). This comparative study
 385 was also extended to two vertebrate canonic opsins present in *Rattus norvegicus* and one non-
 386 echinoderm opsin group in a brachiopod *Lingula anatina*. The three bold boxes highlight the best
 387 similarity percentage between the crinoid opsins and the non-canonical rhabdomeric opsin of *S.*
 388 *purpuratus*. (B) The chromosomal position of the three opsin genes in the *Antedon bifida* genome
 389 represented by a leading arrow indicating the reading direction of the gene. (C) The representation of
 390 intronic and exonic regions, and indication of homologous regions) in the three opsin genes of the
 391 studied species (*A. bifida*) compared to the sea star and sea urchin rhabdomeric opsin genes of the

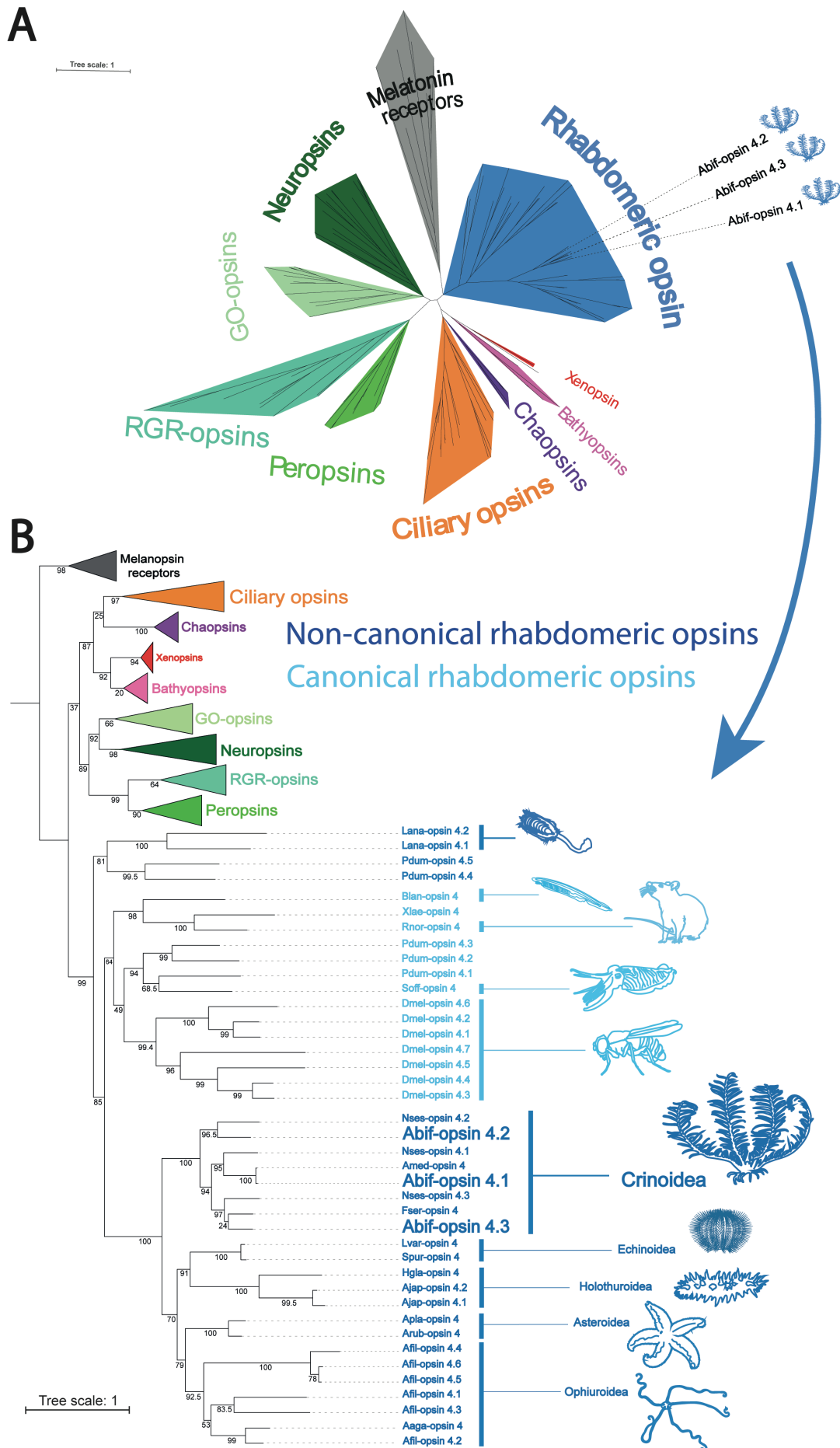
392 model species (*A. rubens* and *S. purpuratus*). (D) Alignments in the third (Tm III) and seventh (Tm VII)
393 transmembrane helix domains as well as in the second extracellular loop (EC II) protein region of the
394 six opsin sequences evidenced in both crinoid species (Abif = *Antedon bifida*; Nses = *Nesometra*
395 *sesokonis*) versus 14 rhabdomeric opsins of other bilaterian metazoans (Arub = *Asterias rubens*; Apla
396 = *Acanthaster planci*; Spur = *Strongylocentrotus purpuratus*; Lvar = *Lytechinus variegatus*; Afil =
397 *Amphiura filiformis*; Blan = *Branchiostoma lanceolatum*; Rnor = *Rattus norvegicus*; Ajap = *Apostichopus*
398 *japonicus*; Hgla = *Holothuria glaberrima*; Dmel = *Drosophila melanogaster*). The first and the last
399 supplementary sequences in these alignments are respectively the rat rhodopsin (a reference ciliary
400 opsin which gives the amino acid numeration) and the melatonin receptor of sea urchin *S. purpuratus*
401 (non-opsin GPCR protein) used as comparison models. Different amino acid patterns, characteristic of
402 typical opsins, are highlighted in colour in these alignments and are all present in the three crinoid
403 opsins.

404

405 **Phylogenetic position of crinoid opsins**

406 A first exploded global opsin phylogeny in different species of Echinoderms and other typical bilaterian
407 phyla allowed it to recover all nine ancestral bilaterian opsin lineages (**Fig. 4A, full phylogenetic tree**
408 **presented in Supplementary Figure S1**). In this way, we were able to confirm *in silico* analyses that all
409 three crinoid opsins belong to the rhabdomeric opsin group (opsins 4). A focus on rhabdomeric opsins
410 4 then allowed us to highlight their relationships between investigated crinoid species and other
411 echinoderms (**Fig. 4B**). Crinoid and other echinoderm rhabdomeric opsins gathered into a well-
412 separated clade (**Fig. 4B**) that further branched apart from classical rhabdomeric opsins like vertebrate
413 melanopsins and *Drosophila* r-opsins, supporting that all rhabdomeric opsins in echinoderms
414 diversified from a unique common ancestor. This is consistent with the fact that all echinoderm opsins
415 4 have so far been identified as non-canonical rhabdomeric opsins and in this phylogeny, appear to be
416 the sister group to the canonical opsins of the chordates and protostomes. Other “non-conventional”
417 rhabdomeric opsins of brachiopods and polychaetes are not directly grouped with echinoderm opsins
418 and are represented as a sister group of the clade containing canonical opsins and non-canonical opsin
419 of echinoderms. It is also important to notice that the three opsin sequences discovered from the
420 genomes of both crinoid species (*Antedon bifida* and *Nesometra sesokonis*) are exclusively grouped
421 with two other published partial opsin sequences from the transcriptomes of two other feather star
422 species. This crinoid opsin clade is placed in the basal position of the other echinoderm rhabdomeric
423 opsins, in agreement with the phylogeny of extant echinoderms. The other echinoderm opsins 4 are
424 also grouped according to the different echinoderm classes, in perfect agreement with the well-
425 established phylogenetic classification of the phylum. The relationships between crinoid opsins point
426 to the existence of three rhabdomeric opsin lineages in the Antedonidae family, the most basal
427 position being occupied by crinoid opsin 4.2 orthologs.

428



430 **Figure 4.** Phylogenetic analysis of Crinoid opsins. (A) Global phylogenetic tree of the nine
431 representative ancestral opsin lineages in bilaterian metazoans supported by maximum likelihood
432 method. Bootstrap values are indicated at the root of each opsin cluster. The melatonin receptor
433 cluster is used to root the phylogenetic tree and the branch length scale gives an insight into the
434 relative rate of amino acid substitution per site. The three opsin sequences evidenced in the crinoid
435 *Antedon bifida* (Abif) are indicated in bold into the rhabdomeric opsin cluster and associated with blue
436 crinoid icons. (B) Focus on the rhabdomeric opsin cluster with a distinction between Canonical (in light
437 blue) and non-canonical (in dark blue) R-opsins. The branch lengths and bootstrap values are indicated
438 in this case respectively above and below the branches. There are in total 40 rhabdomeric opsin
439 sequences present in this phylogeny belonging to 18 representative bilaterian species (Echinoderms:
440 Abif = *Antedon bifida*; Amed = *Antedon mediterranea*; Nses = *Nesometra sesokonis*; Fser = *Florometra*
441 *serratissima*; Arub = *Asterias rubens*; Apla = *Acanthaster plancii*; Spur = *Strongylocentrotus purpuratus*;
442 Lvar = *Lytechinus variegatus*; Afil = *Amphiura filiformis*; Aaga = *Astrotomma agassizii*; Ajap =
443 *Apostichopus japonicus*; Hgla = *Holothuria glaberima*; Chordates: Blan = *Branchiostoma lanceolatum*;
444 Rnor = *Rattus norvegicus*; Xlae = *Xenopus laevis*; Lophotrochozoans: Lana = *Lingula anatina*; Pdum =
445 *Platynereis dumerilii*; Soff = *Sepia officinalis*; Arthropods: Dmel = *Drosophila melanogaster*). The three
446 opsin sequences of the crinoid species (*A. bifida*) (Abif-opsin4.1, 4.2 and 4.3) are highlighted in bold at
447 the base of the non-canonical rhabdomeric opsin cluster of Echinoderms. Accession numbers of all
448 sequences are presented in the Supplementary Table S1. The Full circular phylogeny is presented in
449 the Supplementary Figure S1.

450

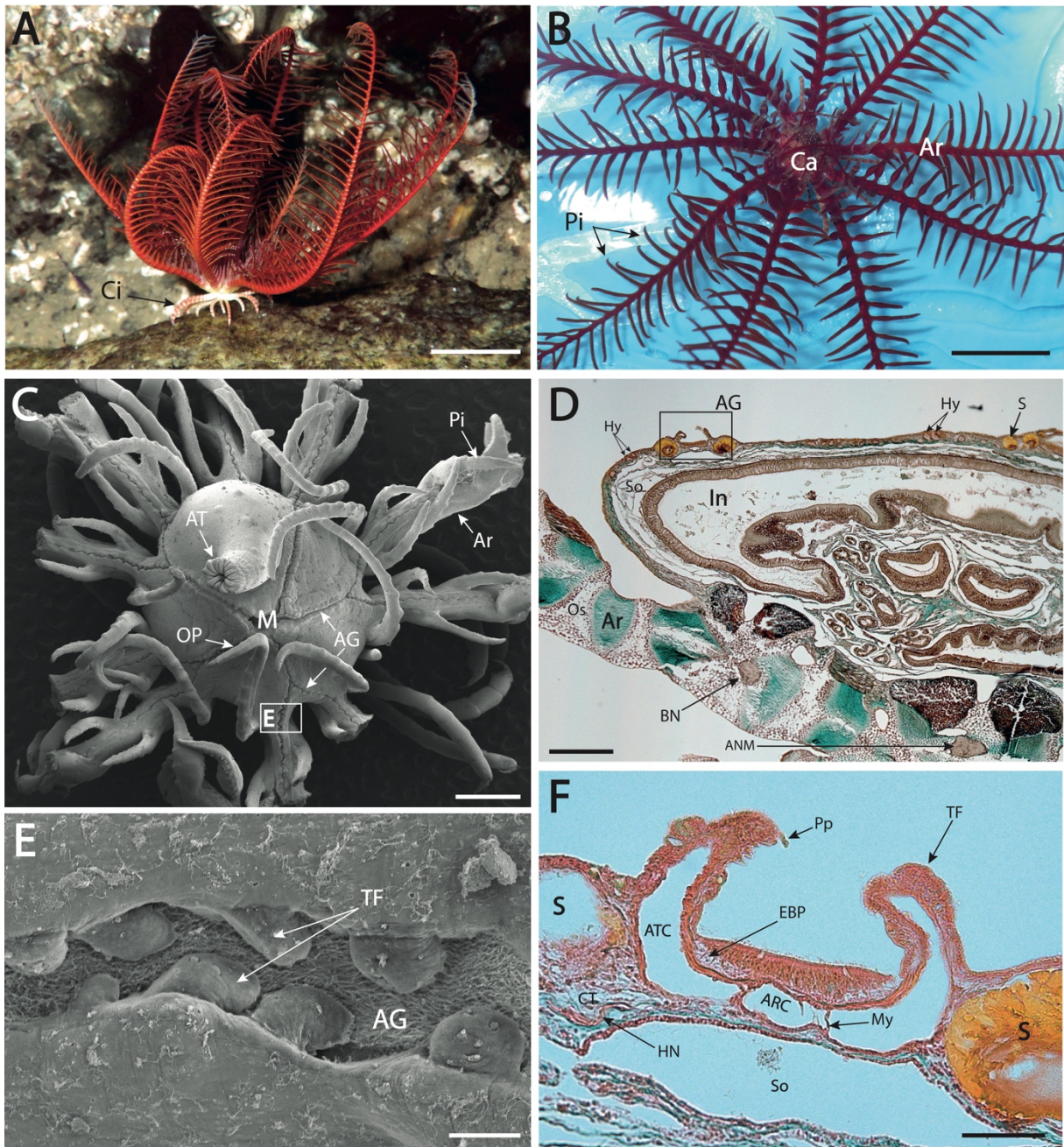
451 ***Antedon bifida* opsins are expressed in the tube feet and nervous systems**

452

453 *Opsin detection in the calyx area*

454 *A. bifida* has a typical morphology of feather star crinoids (*Comatulida*) with a central calyx with mobile
455 hook-like cirri on the aboral side for locomotion (**Fig. 5A**) and ten filtering arms connected to the oral
456 side of the calyx. Each arm possesses numerous bilateral ramifications called pinnules (**Fig. 5B**). A deep
457 aboral nervous system, typical of crinoids, is localised in the deep part of the calyx and constituted by
458 a complex bowl-shaped cluster whose branches form the brachial nerves (**Fig. 5F**). Ramifications of
459 brachial nerves extend into the aboral side of the pinnules. The mouth is in the middle of the calyx oral
460 side (tegmen), right next to the anal tube that is slightly off-centre (**Fig. 5C**). Five ambulacral grooves,
461 that carry filtered food to the mouth, start from the mouth and dichotomise before extending to the
462 arms. Each calyx groove is alternately bordered on both sides by spherical bodies called saccules (**Fig.**
463 **5D-F**) and by a unique series of tube feet (**Fig. 5E-F**). Histological cross-sections of the ambulacral
464 groove region point to the presence of two neuronal networks, on one hand, the ectoneural
465 basiepithelial nerve plexus confined at the base of the groove epidermis and, on the other hand, a
466 diffuse hyponeural nerve plexus present slightly down in the connective tissue (**Fig. 5F**).

467



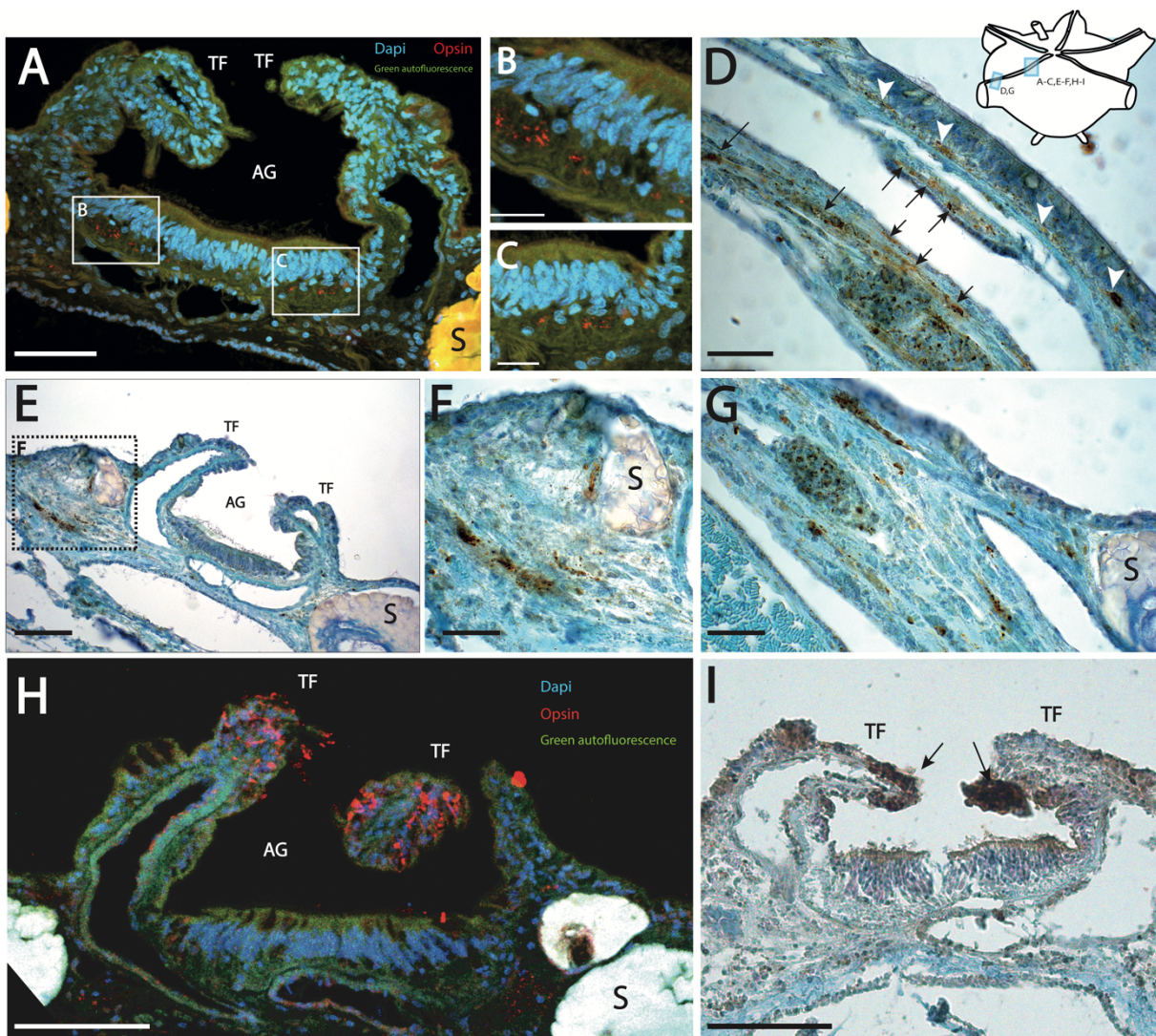
468
 469 **Figure 5.** Morphological structure of the Calyx: (A) An adult specimen of *Antedon bifida*. (B) Oral view
 470 of the central calyx surrounded by the ten branched arms. (C) Scanning electron microscopy picture of
 471 the whole oral surface (tegmen) of the calyx with a focus on the ambulacral groove indicated by a box.
 472 (D) Lateral histological cross section on the global calyx with a focus on the boxed ambulacral groove
 473 groove region. (E) Micrograph of the calycinal groove portion bordered by well-visible tube feet. (F)
 474 Transversal histological section (Masson's trichrome stain) of the ambulacral groove on the calyx. AG:
 475 Ambulacral Groove ; ANM: Aboral Nerve Mass; Ar: Arm; ARC : Ambulacral Radial Canal ; AT: Anal Tube;
 476 ATC: Ambulacral Tentacular Canal; BN: Brachial Nerve; Ca: Calyx; Ci : Cirri; CT : Connective Tissue; EBP:
 477 Ectoneural Basiepithelial Plexus ; HN : Hyponeural Nerve; Hy: Hydropores; In: Intestine; M: Mouth; My:
 478 Myocyte; OP: Oral Pinnule; Os: Ossicle; Pi: Pinnules; Pp: Papilla; S: Sacculae; So: Somatocoele; TF
 479 Tube Foot. Scales: A. 20 mm, B. 10 mm, C. 400 μ m, D. 300 μ m, E. 20 μ m, F. 50 μ m.

480

481 Both ecto- and hyponeuronal plexus exhibited a strong immunoreactivity after exposure to
 482 antibodies raised against opsin 4 of the sea star *Asterias rubens*, supporting the presence of opsins in

483 these nervous structures (**Fig. 6 A-E**). The high sequence similarity between the antigen sequence of
484 *A. rubens* opsin 4 and the sequence of *A. bifida* opsin 4.1 (**Suppl. Fig. S2**) suggests that the
485 immunoreactivity observed both by immunofluorescence (**Fig. 6 A-C**) and by immunohistochemistry
486 (**Fig. 6 B-E**) correspond to the expression of the Abif-opsin 4.1 in these nervous structures.

487 Other structures showing the presence of opsins corresponded to tube feet, bordering the
488 ambulacral grooves (**Fig. 5 E-F**). The epidermis of each tube foot presents several papillae with ciliary
489 sensory cells. The opsin immunoreactivity was observed more precisely in the epidermal cells at the
490 base and tip of these sensory papillae (**Fig. 6 F-G**). These immunodetections were performed with
491 antibodies raised against *A. rubens* opsin 1.1. The similarity of antigenic sequence between *A. rubens*
492 opsin 1.1. and *A. bifida* opsin 4.2 (**Suppl. Fig S2**) suggests that the immunoreactivity observed in the
493 papillae of tube feet corresponds to the expression of the Abif-opsin 4.2. However, sequence
494 divergence for the target binding region in the available peptide antibodies does not rule out that opsin
495 4.3 may co-localise with opsin 4.2 or be expressed in additional sensory cells.
496



497
498 **Figure 6.** Immunostainings of two rhabdomeric opsins in the Calix ambulacral groove tissues of
499 *Antedon bifida*: (A) Localisation of opsin 4.1 by red immunofluorescence into the ectoneural
500 basiepithelial nerve plexus just under the ambulacral groove epithelium. (A-I; AII) Focus on the two
501 basiepithelial spots of opsin labelling in red. (B) Opsin 4.1 is highlighted at the base of arm with a
502 localisation on the one hand in the ectoneural basiepithelial plexus (white head arrow) and the other
503 hand in the hyponeural plexus present deeper into the connective tissue (black arrow). (C) Localisation

504 of the same opsin 4.1 by immunocytochemistry in brown into the hyponeural nerve plexus inside the
505 connective tissue of the calyx ambulacral groove. (D) Focus on the hyponeural opsin showing the
506 localisation near a saccule. (E) Focus on the brown immunostaining of opsin 4.1 in the hyponeural
507 plexus of the base of the arm. (F) Labelling in red by immunofluorescence of opsin 4.2 at the top of
508 tube feet (in the sensory papillae) bordered the ambulacral groove of the calyx. (G)
509 Immunocytochemistry showing the opsin 4.2 expression at the top of tube feet (arrow). Scales: A.
510 50µm, A'-A''. 10µm, B. 25µm, C. 50µm, D. 20µm, E. 20µm, F. 50µm, G. 50µm.

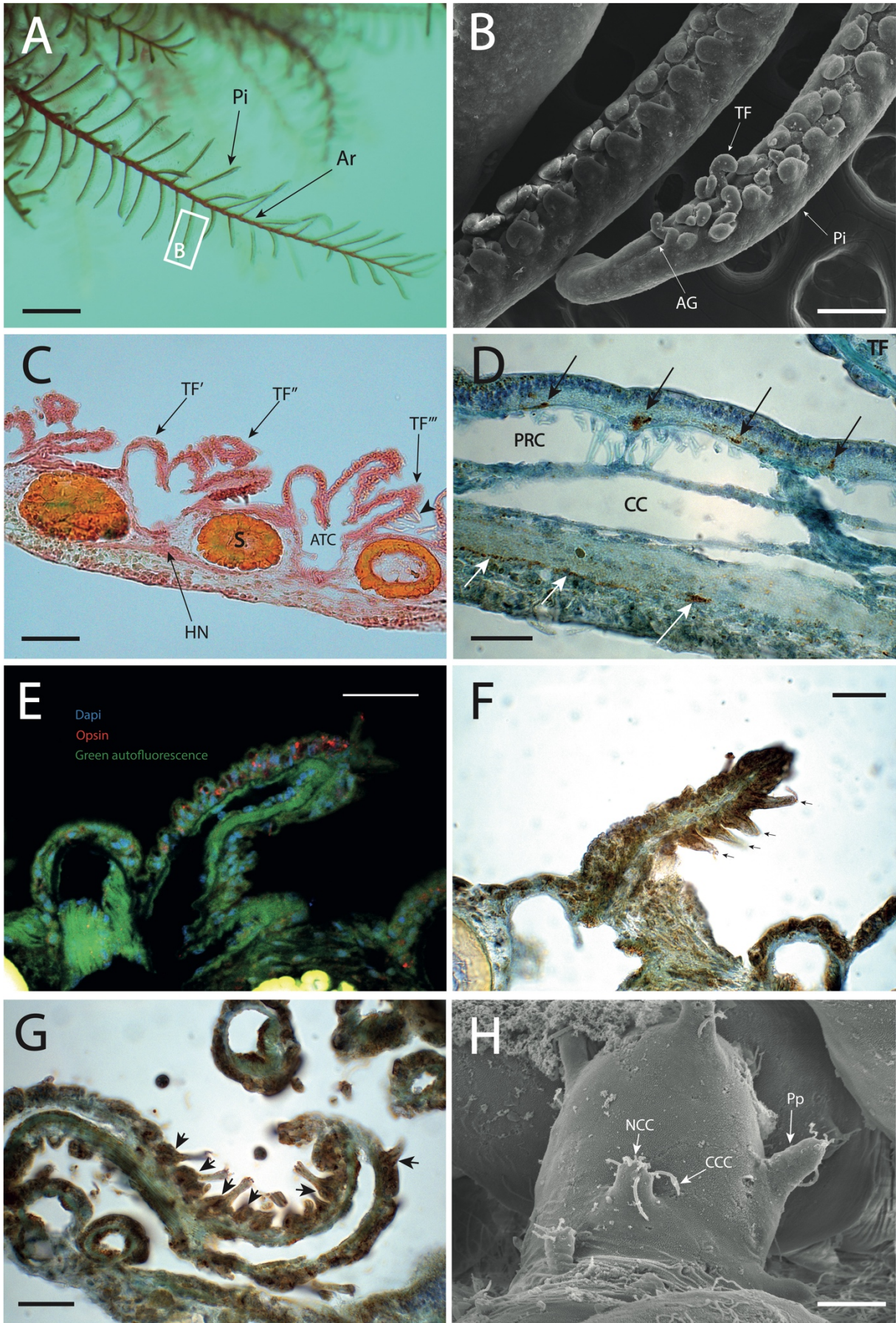
511

512 *Opsin detection in the pinnules*

513 The pinnules of crinoids are lateral extensions of the arms (**Fig. 7 A**). A pinnular ambulacral
514 groove occupies the middle oral side of each pinnule and is bordered by two rows of tube feet allowing
515 food capture and transport (**Fig. 7 B**). The pinnular tube feet are grouped in triads arranged
516 alternatively on either side of the groove (**Fig. 7 C**). These triads consist of one long primary tube foot
517 and a medium-sized secondary tube foot dedicated to trap food particles, and a short tertiary tube
518 foot whose function is to form the food bolus that is transported to the mouth [Lahaye and Jangoux
519 1985]. Similarly to the calyx tube feet, pinnular tube feet also have several epidermal sensory-secretory
520 outgrowths called papillae. Papillae are known to feature several cell types: secretory cells, peripheral
521 support cells with a long apical cilium, and central neurosensory cells with a shorter cilium [Flammang
522 and Jangoux 1991]. Scanning electron microscopy observations highlighted ciliary structures at the
523 extremity of the papillae (**Fig. 7 H**). As for the case in calyx papillae, these pinnular papillae showed an
524 immunoreactivity with the anti-Arub_opsin 1.1 antibodies (**Fig. 7 E-G**). These opsin labelling
525 corresponds more probably to the expression of Abif-opsin 4.2 as mentioned above (**Suppl. Fig. S2**).
526 The labelling was strong in the basal part of papillae but was also present occasionally in the apical
527 pole of papillae cells (**Fig. 7 E-G**).

528 The three parts of the pinnular nervous system are extensions of those found in the arms and
529 calyx. The pinnular ambulacral grooves feature an ectoneural basiepithelial plexus and a deep aboral
530 nerve plexus in the centre of the pinnules. On the other hand, the hyponeural nerve plexus is
531 constituted by two lateral nerve cords that run longitudinally on either side of the pinnules and
532 innervate the tube feet and saccules (**Fig. 7C**). As was the case in the calyx section, aboral, ectoneural
533 and hyponeural networks present in pinnules expressed opsin proteins (**Fig. 7D**). As mentioned before
534 this immunostaining in nervous structures corresponds, more probably, to the presence of Abif-opsin
535 4.1 (**Suppl. Fig. S2**).

536



539 **Figure 7.** Anatomical structures of pinnules tissues and rhabdomeric opsin immunostainings in the
540 pineal ambulacral groove in *Antedon bifida*: (A) Crinoid arm with a focus on a pinnule indicated by a
541 red box. (B) Scanning electron microscopy picture at the extremity of the pinnule. (C) Longitudinal
542 histological section (Masson's trichrome stain) in the lateral pinnule edge. (D) Localisation of opsin 4.1
543 in the ectoneural basiepithelial plexus (dark arrow) and the deep aboral nerve of the pinnule (white
544 arrow). These histological structures become visible thanks to the further longitudinal section in the
545 centre of the ambulacral groove. (E) Labelling of opsin 4.2 by immunofluorescence in red into the tube
546 feet epidermis and the extremity of sensory papillae. (F) Immunostaining (brown precipitate) of opsin
547 4.2 in the lateral sensory papillae (dark arrow) of one secondary tube foot. (G) Similar opsin 4.2
548 immunostainings in brown at the base of sensory papillae (dark arrow) of one primary tube foot. (H)
549 Micrography of the sensory papillae structures of a tube foot. AG: Ambulacral groove; Ar: Arm; ATC:
550 Ambulacral Tentacular Canal; CC: Coelomic Canal; CCC: Covering ciliary cell; NCC: Neuronal Ciliary Cell;
551 Pi: Pinnules; TF: Tube foot; TF'/TF''/TF''': primary/secondary/tertiary Tube Foot; HN: Hyponeural
552 nerve; Pp: Papilla; PRC: Pinnule Radial Canal. Scales: A. 5mm, B. 200µm, C. 50µm, D. 20µm, E. 20µm,
553 F. 20µm, G. 20µm, H. 3µm.

554

555 Discussion

556

557 *Crinoid light behaviour*

558 Multiple reef-dwelling Comatulid species feed mainly at night and hide in rocky crevices or fold their
559 arms and pinnules during the day which suggests photophobic behaviours [Magnus 1962; Meyer 1973;
560 Rutman and Fishelson 1969]. Our results evidenced a negative phototactic behaviour in *Antedon bifida*
561 which is consistent with previous *in situ* observations of hiding behaviour made in other shallow water
562 feather stars. One study also mentioned a positive phototactic behaviour for a small feather star
563 species *Dorometra nana* that was attracted to a light source [Clark 1909]. This isolated observation
564 could indicate a species-specific response, but the photic response could also be affected by different
565 variables such as the light intensity. Some observations suggested that the nocturnal feeding activity
566 and the diurnal shelter-seeking behaviour of many crinoids are not linked to the circadian cycle but
567 would be well induced by direct ambient light detection. Indeed, some specimens belonging to the
568 same species (*Heterometra savignii*) but living at greater depths, in an environment of constant low
569 luminosity, tended rather to lose their nocturnal activity but kept their high photophobic reaction to
570 an intense light stimulus [Fishelson 1974]. It is therefore not surprising that the studied population of
571 *A. bifida* living just below the surface, clinging to the shade under pontoons of the marina, flees the
572 polychromatic white light as it was previously reported in the literature based on observations in
573 natural conditions [Dimelow 1958].

574 The ethological tests carried out on *Antedon bifida* showed that the negative phototactic
575 behaviour reached its maximum amplitude for blue light pointing to the greater sensitivity of this
576 species for the short light wavelength range ($\lambda_{\max} = 463$ nm). The greater sensitivity to blue light has
577 also been demonstrated several times by phototactic behavioural tests in other echinoderm groups,
578 such as the sea urchin *Strongylocentrotus purpuratus* [Ullrich-Lüter et al 2011], the brittle star
579 *Amphiura filiformis* [Delroisse et al 2014] and, more recently, the sea cucumber *Holothuria leucospilota*
580 [Wang et al 2023]. The blue part of the light spectrum is the wavelength range that penetrates the
581 farthest into the water column and is, therefore, the light component, together with green light, mostly
582 present in open water environments (Davis 1991). Electrophysiological studies in ocellary structures
583 of some reef-dwelling sea star species attested a very narrow sensitivity peak for the blue wavelength
584 (450 nm) suggesting the presence of a blue-sensitive opsin in ocellary spots of these sea stars [Garm
585 and Nilsson 2014, Petie et al. 2016]. By contrast, *A. bifida* is sensitive to a much broader light spectrum.

586 Experiments performed in the present study demonstrated a significant negative phototactic
587 behaviour for red light ($\lambda_{\max} = 630\text{nm}$). This sensitivity to red light may be correlated with the fact that
588 this species lives at very shallow depths (less than 10m) and therefore is exposed to longer wavelengths
589 like red penetrating only a few metres below the sea surface, especially in the Atlantic and North Sea
590 where the light intensity declines quickly with depth (Davis 1991, Capuzzo et al. 2013, 2015). This large
591 variability in the range of perceived light wavelengths, together with specific expression patterns,
592 suggests that directional photoreception in this species of Comatulida may be mediated by different
593 opsins. Our study confirms the presence of three different opsin genes evidenced in the genome of *A.*
594 *bifida*, bearing all conserved characteristics of functional opsins. This suggests that *A. bifida* relies on
595 rhabdomeric opsins for extraocular light perception. Another clue pointing to the presence of a multi-
596 opsin photoreception in *A. bifida* is the expression of two different rhabdomeric opsins localised in
597 specific tissues such as the subepidermal ectoneural nerve plexus and the tips of tube feet. However,
598 further *in vitro* investigations of the bioactivity of the three different opsins are required to functionally
599 characterise the crinoid opsins.

600 A trend for *A. bifida* to move away from the light source was also observed for green light
601 ($\lambda_{\max} = 512\text{ nm}$), but this was not significant. This lack of significance is probably due either to a low
602 detection of green light or to a lack of phototactic behavioural response for this wavelength in this
603 Comatulid species. Green light is the wavelength range most present in the shallow coastal waters
604 where *A. bifida* populations are found. This ecologically relevant green wavelength could therefore
605 lead to distinct behavioural responses in contrast to other light wavelengths. A similar absence of
606 reactivity to green light has already been described in tadpoles of the amphibian species *Xenopus laevis*
607 living in green eutrophic water [Roberts et al. 2000]. Nevertheless, future behavioural tests with green
608 light wavelength could be carried out on a larger number of individuals to ensure that there has been
609 no statistical bias due to insufficient sampling.

610

611 ***Opsin evolution in feather stars***

612 *In-silico* analyses performed on the genome of the crinoid species *A. bifida* and *N. sesokonis* have
613 revealed the presence of only three opsin genes. In the chromosome-scale genome of *A. bifida*, the
614 opsin genes are distributed on chromosomes 4 and 6. All three opsin genes were identified as
615 belonging to the same group of non-canonical echinoderm rhabdomeric opsins. This low opsin gene
616 diversity was quite unexpected given that the other four echinoderm classes possess a much more
617 varied opsin repertoire with between 9 and 15 different opsin genes currently known [D'Aniello et al.
618 2015]. For instance, sea urchins and brittle stars, still exhibit seven of the nine ancestral opsin lineages
619 inherited from the common ancestor of bilaterians: ciliary opsins, bathyopsins, Go-opsins, non-
620 canonical rhabdomeric opsins, chaopsins, peropsins/RGR-opsins and neuropsins [Ramirez et al. 2016].

621 Crinoids are considered as the basal lineage of echinoderms which generally justified their
622 importance in comparative evolutionary studies. Crinoidea has a long evolutionary history of at least
623 485 million years [Rouse et al. 2013; Oji and Twitchett 2015] and all crinoids living today originated
624 from the single branch of Articulata, the only crinoid lineage to have survived the great extinction of
625 the late Paleozoic [Baumiller et al. 2011]. Current feather stars therefore represent a relatively derived
626 group compared to the ancestral forms of the Paleozoic. The Crinoidea available genomes (i.e.,
627 *Anneissia japonica* [ASM1163010v1 in NCBI, 0.5896 Gb], *Nesometra sesokonis* [ASM2563120v1 in NCBI,
628 0.5971 Gb] and *Antedon bifida* [ecAntBif1.1 in NCBI, 0.3196 Gb] the only chromosome-scale genome)
629 are comparable to sea stars (e.g., *Asterias rubens* (0.4176 Gb) and *Marthasterias glacialis* (0.52Gb)
630 [Parey et al. 2024]) but appear considerably smaller compared to other echinoderm genomes (e.g.,
631 *Strongylocentrotus purpuratus* (0.9218 Gb), *Holothuria leucospilota* (1.4 Gb), and *Amphiura filiformis*
632 (1.57 Gb) [Parey et al. 2024]). In *A. bifida*, specifically, a reduced number of chromosomes is observed
633 (11 chromosomes) compared to other chromosome-scale echinoderm genomes (i.e., 18 for

634 *Paracentrotus lividus* [Parey et al. 2024], 22 for *A. rubens*, 23 for *H. leucospilota* and 20 for *A. filiformis*
635 [Parey et al. 2024]). Our study further reveals a reduced opsin repertoire accompanying these genomic
636 characteristics. It is possible that, during their evolutionary history, these modern crinoids (many live
637 at relatively great depths in low luminosity) may have lost many of the ancestral opsin groups still
638 present in other echinoderms. The smaller crinoid genome could also explain the lower number of
639 intronic regions in their opsin genes, making crinoid opsin genes shorter than those found in other
640 echinoderm classes.

641 However, the presence of a single bilaterian opsin class may not be generalisable to all crinoid
642 groups but may just be specific to the Comatulida family Antedonidae. Indeed, the two species (*A.*
643 *bifida* and *N. sesokonis*), whose genomes have been investigated in the present study, belong to the
644 family Antedonidae. Research carried out on the only other available crinoid genome belonging to the
645 Comatulidae family species (*Anneissia japonica*) revealed no opsin gene. A more complete sampling
646 across Crinoidea will be crucial to have a more complete representation of opsin diversity within the
647 class.

648 The alignment comparisons with other metazoan rhabdomeric opsins have demonstrated that
649 all three crinoid protein sequences possess the set of amino acid residues characteristic of functional
650 opsins allowing interaction with both retinal and the G-protein. This suggests that these three
651 rhabdomeric opsins potentially play a direct role in light detection in *A. bifida*. Our behavioural tests
652 support the view that *A. bifida* individuals possess photosensitivity covering a wide part of the light
653 spectrum, potentially related to the activity of different opsins exhibiting distinct spectral absorptions.
654 The involvement of rhabdomeric opsins as the main photoreception molecular actor in the light
655 detection has been mentioned several times in other Echinoderms [Ullrich-Lüter et al 2011; Delroisse
656 et al 2014] notably for sea stars which possess a largely predominant expression of a rhabdomeric
657 opsin in their compound ocelli (optic cushion) at the end of arms [Lowe et al. 2018].

658 The phylogenetic analysis of rhabdomeric opsins in bilaterians places the three crinoid opsins
659 together at the base of the non-canonical rhabdomeric opsin clade of Echinoderms. Within the latter,
660 the relationship of opsins belonging to the different classes follows perfectly the classical phylogenetic
661 classification of Echinoderms, as highlighted in other studies [Delroisse et al. 2014; D'Aniello et al.
662 2015; Lowe et al. 2018]. The fact that the three crinoid opsins are clustered together suggests that
663 they come from a duplication of an ancestral rhabdomeric opsin gene in this group. The same more
664 extended gene polyplication was observed in the brittle star species *Amphiura filiformis*, which has 6
665 different rhabdomeric opsin genes [Delroisse et al 2014].
666

667 **Potential photosensory structures in crinoids**

668 Opsin immunostaining revealed the presence of at least two opsins in various tissue structures
669 associated with the ambulacral grooves of the calyx and pinnules. One opsin was associated with the
670 different nerve plexi whereas another opsin was expressed at the tips of the tube feet. These
671 histological structures containing opsins are ideally located on the surface of the body and face away
672 from the substratum, allowing a maximum detection of the sunlight rays.

673 The first opsin detected in the nervous plexus by antibodies raised against opsin 4 from the
674 sea star *Asterias rubens* very likely corresponds to opsin 4.1 of *A. bifida*. Indeed, as evidenced by the
675 alignments of the protein region recognised by the antibody, *A. bifida* opsin 4.1 shows the highest
676 percentage (46.66%) of similarity with the epitope sequence of *Asterias rubens* rhabdomeric opsin (see
677 the alignment in **Suppl. Fig. S2**). The presence of rhabdomeric opsins directly linked to the nervous
678 system is relatively well described in other echinoderms, notably in the radial nerves and sensory
679 nerves innervating the tube feet in sea urchins and brittle stars [Ullrich-Lüter et al 2011; Delroisse et
680 al 2014]. It is well known that the ectoneural basiepithelial nerve plexus of echinoderms is involved in
681 the transmission of sensory information [Weber and Grosmann 1977; García-Arrarás et al 2001;

682 Mashanov et al 2023; Adameyko 2023], suggesting that this nervous plexus may also be involved in
683 transmitting photo-sensorial information. By contrast, a photosensory activity within the hyponeural
684 plexus is more intriguing. Indeed, this nervous plexus, located deeper in the connective tissue, is
685 generally considered to perform only motor functions in echinoderms [García-Arrarás et al 2001].
686 Nevertheless, some paleontological studies have demonstrated that the hyponeural nerves in
687 Paleozoic crinoids Camerata innervated directly some specific sensory organs in the calyx [Haugh
688 1978], demonstrating a possible dual sensory-motor role in crinoids, including a possible role for opsins
689 in these deeper nerve fibres.

690 The detection of opsins in hyponeural nerves could shed new light on the still-unknown
691 function of the saccules present below the surface of crinoid pinnules. These spherical bodies are
692 highly refractive [Mallefet et al 2023] and are quite abundant in some species of feather stars, such as
693 our study model *Antedon bifida*. They are regularly arranged under the epidermis on either side of the
694 ambulacral grooves in the calyx and pinnules. The exact function of these saccules is still unknown, but
695 numerous hypotheses about their physiological role have already been proposed, such as mucus
696 secretion [Carpenter 1884; Clark 1921; Mironov and Pawson 2010], as an energy reserve [Hyman 1955]
697 or playing a role in light production in bioluminescent species [Mallefet et al 2023]. Because of their
698 optical properties, a hypothesis has been formulated suggesting their possible role as refractive lenses
699 enabling light rays to converge on photoreceptors [Holland 1967]. The expression of rhabdomeric
700 opsins in the hyponeural plexus located under the saccules, and innervating them, seems to support
701 this hypothesis.

702 Earlier studies have also highlighted the presence of numerous pigments in the subepithelial
703 connective tissue of *A. bifida* ambulacral grooves, as well as in other feather stars [Carpenter 1876,
704 Dimelow 1958]. This pigmentation could potentially play a shading role at the level of ecto- and
705 hyponeural nerve *plexi* expressing opsins. This shading system would be necessary to allow a
706 directional photoreception, as demonstrated by phototactic tests in *A. bifida*.

707 The second opsin was specifically localised in the epidermis of the tube feet bordering the
708 ambulacral grooves of the calyx and pinnules. This opsin was immunodetected using a different rabbit
709 antibody raised against *Asterias rubens* opsin 1.1. Although this antibody recognises a ciliary opsin in
710 the sea star, the epitope sequence shows a relatively high similarity with the opsin 4.2 from *A. bifida*
711 (62.5%, **Suppl. Fig. S2**). Furthermore, a search for sequence homology has been performed against the
712 entire *A. bifida* genome. Our results indicate that Abif-opsin 4.2 has a significant similarity (62.5%)
713 with the sequence of the immunogenic peptide used to produce antibodies against sea star opsin 1.1.
714 In the future, the results will need to be confirmed using immunoblots analyses.

715 Observing rhabdomeric opsin expression in tube feet of *A. bifida* is noteworthy, given that r-
716 opsin localisation in tube feet has been previously demonstrated in other echinoderm classes such as
717 sea urchins and brittle stars [Ullrich-Lüter et al 2011, Delroisse et al 2014], yet not in crinoids thus far.
718 In contrast to other echinoderms, crinoids have their tube feet facing away from the substratum, which
719 exposes them more effectively to light in the water column. Additionally, ciliary neurosensory cells
720 have been found in various epidermal extensions such as “papillae” and “hillocks” of crinoid tube feet
721 [Flammang and Jangoux 1991]. The opsin immunoreactivity is precisely located both at the base and
722 occasionally at the tip of these sensory papillae, suggesting that these sensorial structures may be
723 involved in light perception. This potential tube foot photoreception is corroborated by *pax 6* gene
724 expression observed in the tube foot tips of the feather star species *Anneissia japonica* [Omori et al
725 2020], suggesting the probable presence of photoreceptors at the tips of tube feet in crinoids.
726 Expression of *pax 6* is generally recognised for its pivotal role in the embryonic development of light-
727 sensitive structures across bilaterian metazoans [Callaerts et al. 1997; Gehring and Ikeo 1999; Arendt;
728 2003; Zuber et al. 2003; Martínez-Morales et al. 2004; Stierwald et al. 2004; Kozmik 2005].
729 Interestingly, *pax 6* has also been shown to be expressed in adult photoreceptor organs in various

730 echinoderms, including co-expression of *pax 6* and opsin genes in the sea urchin species *S. purpuratus*
731 [Ullrich-Lüter et al 2011]. However, it will be necessary to, e.g., express and characterise the function
732 of these opsins by heterologous expression and develop gene knock-out workflows in this new model
733 system to fully demonstrate the role and molecular mechanisms underlying non-canonical
734 rhabdomeric opsins photoreception.

735

736 **Funding**

737 YN and ED are supported by FRIA grants from the “Fonds de la Recherche Scientifique” of Belgium
738 (F.R.S.-FNRS) and a PDR grant (T.0169.20). AL was supported by a FRIA grant from the F.R.S.-FNRS. JD
739 is a postdoctoral researcher funded by a PDR project from the F.R.S.-FNRS (T.0071.23). PF is research
740 director from the F.R.S.-FNRS.

741

742 **Acknowledgements**

743 This study contributes to the BioSciences Research Institute from the University of Mons and the
744 “Centre Interuniversitaire de Biologie Marine” (CIBIM). The authors are grateful to the staff of the
745 Marine Station of Concarneau for help and support.

746

747 **Conflict of interest**

748 The authors declare no conflicts of interest.

749

750 **Author contributions**

751 YN, IE, JD collected samples. YN, ML, AL, LV and JD performed the experiments. YN and JD analysed
752 and interpreted the results. YN and JD prepared the first draft of the manuscript. JD and PF supervised
753 the study. All authors read and approved the final manuscript.

754

755 **Data availability**

756 Data generated/analysed during the current study are available from the corresponding author upon
757 reasonable request.

758

759 **References**

- 760 Adameyko I. (2023). Evolutionary origin of the neural tube in basal deuterostomes. *Current Biology* 33:
761 R319–R331 (2023). <https://doi.org/10.1016/j.cub.2023.03.045>
- 762 Arendt D. (2003). Evolution of eyes and photoreceptor cell types. *Int J Dev Biol.* 47(7-8): 563-571
763 (2003). PMID: 14756332.
- 764 Baumiller TK, Salamon MA, Gorzelak P, Mooi R, Messing CG, Gahn FJ. (2010). Post-Paleozoic crinoid
765 radiation in response to benthic predation preceded the Mesozoic marine revolution. *Proc Natl Acad*
766 *Sci U S A.* Mar 30;107(13):5893-6 (2010). <https://doi.org/10.1073/pnas.0914199107>
- 767 Berrill M. (1966). The ethology of the Synaptid holothurian, *Opheodesoma spectabilis*. *Canadian*
768 *Journal of zoology*, 44: 457-482 (1966). <https://doi.org/10.1139/z66-046>
- 769 Burge, C. and Karlin, S. (1997) Prediction of complete gene structures in human genomic DNA. *J. Mol.*
770 *Biol.* 268, 78-94 (1997). <https://doi.org/10.1006/jmbi.1997.0951>
- 771 Callaerts P., Halder G., Gehring W.J. (1997). Pax-6 in development and evolution. *Annu Rev*
772 *Neuroscience* 220: 483–532 (1997). <https://doi.org/10.1146/annurev.neuro.20.1.483>
- 773 Capuzzo E, Painting SJ, Forster RM, Greenwood N, Stephens DT, Mikkelsen O (2013) Variability in the
774 sub-surface light climate at ecohydrodynamically distinct sites in the North Sea. *Biogeochemistry*, 113,
775 85–103 (2013). <https://doi.org/10.1007/s10533-012-9772-6>

- 776 Capuzzo, E., Stephens, D., Silva, T., Barry, J. and Forster, R.M. (2015), Decrease in water clarity of the
777 southern and central North Sea during the 20th century. *Glob Change Biol*, 21: 2206-2214 (2015).
778 <https://doi.org/10.1111/gcb.12854>
- 779 Carpenter P.H. and von Graff L. (1884). On three new species of Metacrinus. Transactions of the
780 Linnean Society of London, 2nd Series, Zoology, 2(14) : 435-446 (1884).
781 <https://doi.org/10.1111/j.1096-3642.1885.tb00296.x>
- 782 Carpenter, P.H. (1885) Report upon the Crinoidea collected during the voyage of H.M.S. Challenger
783 during the years 1873-1876. Part I - General morphology of the stalked crinoids. Report of the Scientific
784 Results of the Exploring Voyage H.M.S. Challenger, London, Zoology, 11 (32): 1-442 (1885).
- 785 Clark A. H. (1909). New genera and higher groups of unstalked crinoids. Proceedings of the Biological
786 Society of Washington 22: 173-177 (1909).
- 787 Clark A. H. (1921). A monograph of the existing crinoids, vol. 1 . The comatulids, pt. 2: [General].
788 Bulletin of the United States National Museum. 1-795 (1921).
789 <https://doi.org/10.5479/si.03629236.82.2>
- 790 Clarke D.N., Formery L. and Lowe C.J. (2024). See-Star: a versatile hydrogel-based protocol for clearing
791 large, opaque and calcified marine invertebrates. *BMC EvoDevo* 15:8 (2024).
792 <https://doi.org/10.1186/s13227-024-00228-0>
- 793 Cobb, J. L. S. and Hendler, G. (1990). Neurophysiological characterisation of the photoreceptor system
794 in a brittlestar, *Ophiocoma wendtii* (Echinodermata: Ophiuroidea). *Comp. Biochem. Physiol. A* 97, 329-
795 333 (1990). [https://doi.org/10.1016/0300-9629\(90\)90619-4](https://doi.org/10.1016/0300-9629(90)90619-4)
- 796 D'Aniello S., Delroisse J., Valero-Gracia A., Lowe E.K., Byrne M., Cannon J.T., Halanych K.M., Elphick
797 M.R., Mallefet J., Kaul-Strehlow S., Lowe C.J., Flammang P., Ullrich-Lüter E., Wanninger A., Arnone M.I.
798 (2015). Opsin evolution in the Ambulacraria. *Mar. Genomics*, 24 (2) :177-183 (2015).
799 <https://doi.org/10.1016/j.margen.2015.10.001> Epub 2015 Oct 23. PMID: 26472700
- 800 Davis R. A.(1991). In *Oceanography: An Introduction to the Marine Environment*, 2nd ed. Dubuque, IA:
801 Wm. C. Brown Publishers, 1991.
- 802 Delroisse J., Lanterbecq D., Eeckhaut I., Mallefet J. and Flammang P. (2013). Opsin detection in the sea
803 urchin *Paracentrotus lividus* and the sea star *Asterias rubens*. *Cahiers de Biologie Marine*, 54: 721-727
804 (2013). <http://hdl.handle.net/2078.1/134949>
- 805 Delroisse, J., Mallefet, J., Flammang, P. and Ullrich-Lüter, E. (2014). High opsin diversity in a non-visual
806 infaunal brittle star. *BMC Genomics*, 15: 1035 (2014). <https://doi.org/10.1186/1471-2164-15-1035>
- 807 Delroisse, J., Mallefet, J. and Flammang, P. (2016). De novo adult transcriptomes of two European
808 brittle stars: spotlight on opsin-based photoreception. *PLoS ONE*, 11(4): e0152988 (2016).
809 <https://doi.org/10.1371/journal.pone.0152988>
- 810 Dimelow E. (1958). Pigments Present in Arms and Pinnules of the Crinoid, *Antedon bifida* (Pennant).
811 *Nature* 182, 812 (1958). <https://doi.org/10.1038/182812a0>
- 812 Flammang P. and Jangoux M. (1991). The sensory-secretory structures of the podia of the comatulid
813 crinoid *Antedon bifida* (Echinodermata). In *Echinoderm Research 1991*, L. Scalera-Liaci & C.Caniccatti
814 (eds) 1992 Balkema, Rotterdam. ISBN 90 5410 049 4.
- 815 Fishelson L. (1974). Ecology of northern Red Sea crinoids and their epi- and endozoic fauna. *Marine*
816 *Biology* 26:183–192 (1974). <https://doi.org/10.1007/BF00388888>
- 817 Fritze O., Filipek S., Kuksa V., Ernst O. (2003). Role of the conserved NPxxY(x)5,6F motif in the rhodopsin
818 ground state and during activation. *PNAS*, 100(5): 2290-2295 (2003).
819 <https://doi.org/10.1073/pnas.0435715100>
- 820 García-Arrarás J. E., Rojas-Soto M., Jiménez L. B., Díaz-Miranda L. (2001). The Enteric Nervous System
821 of Echinoderms: Unexpected Complexity Revealed by Neurochemical Analysis. *J Exp Biol* 204 (5): 865–
822 873 (2001). <https://doi.org/10.1242/jeb.204.5.865>

- 823 Garm A, Nilsson DE. (2014). Visual navigation in starfish: first evidence for the use of vision and eyes in
824 starfish. *Proc. Biol. Sci.* 281(1777):20133011 (2014). <https://doi.org/10.1098/rspb.2013.3011> PMID:
825 24403344; PMCID: PMC3896028.
- 826 Gehring W.J. and Ikeo K. (1999). Pax 6: mastering eye morphogenesis and eye evolution. *Trends Genet.*
827 15(9): 371-377 (1999). [https://doi.org/10.1016/s0168-9525\(99\)01776-x](https://doi.org/10.1016/s0168-9525(99)01776-x) PMID: 10461206.
- 828 Gehring W. J. (2005). New Perspectives on Eye Development and the Evolution of Eyes and
829 Photoreceptors, *Journal of Heredity*, 96(3): 171–184 (2005). <https://doi.org/10.1093/jhered/esi027>
- 830 Haugh B. N. (1978). Biodynamic and phyletic paradigms for sensory organs in camerate crinoids.
831 *Lethaia* 11 (2) :145–173 (1978). <https://doi.org/10.1111/j.1502-3931.1978.tb01300.x>
- 832 Holland N. D. (1967). Some observations on the saccules of *Antedon mediterranea* (Echinodermata,
833 crinoidea). *Pubblicazioni Stazione Zool. Napoli* 35, 257–262.
- 834 Hyman L.H. (1955) *The invertebrates, vol IV, Echinodermata*. McGraw-Hill (eds), New York.
- 835 Johnsen S. (1997) Identification and Localization of a Possible Rhodopsin in the Echinoderms *Asterias*
836 *forbesi* (Asteroidea) and *Ophioderma brevispinum* (Ophiuroidea). *Biological Bulletin*. 193: 97-105
837 (1997). <https://doi.org/10.2307/1542739>
- 838 Katoh k., Rozewicki J., Yamada K.D. (2019). MAFFT online service: multiple sequence alignment,
839 interactive sequence choice and visualization. *Briefings in Bioinformatics*, 20(4): 1160–1166 (2019).
840 <https://doi.org/10.1093/bib/bbx108>
- 841 Kozmik Z. (2005). Pax genes in eye development and evolution. *Curr. Opin. Genet. Dev.* 15: 430–438
842 (2005). <https://doi.org/10.1016/j.gde.2005.05.001>
- 843 Lahaye M.C. and Jangoux M. (1985). Functional morphology of the podia and ambulacral grooves of
844 the comatulid crinoid *Antedon bifida* (Echinodermata). *Marine Biology* 86, 307-318 (1985). Doi:
845 [10.1007/bf00397517](https://doi.org/10.1007/bf00397517)
- 846 Lam-Tung Nguyen, Heiko A. Schmidt, Arndt von Haeseler, and Bui Quang Minh (2015) IQ-TREE: A fast
847 and effective stochastic algorithm for estimating maximum likelihood phylogenies. *Mol Biol Evol*,
848 32:268-274 (2015). <https://doi.org/10.1093/molbev/msu300>
- 849 Lowe EK, Garm A.L., Ullrich-Lüter E., Cuomo C., Arnone M.I. (2018). The crowns have eyes: multiple
850 opsins found in the eyes of the crown-of-thorns starfish *Acanthaster planci*. *BMC Evol. Biol.*, 18(1):168
851 PMID: 30419810 (2018). <https://doi.org/10.1186/s12862-018-1276-0>
- 852 Li Y.Y., Su F.J., Hsieh Y.J., Huang T.C. and Wang Y.S. (2021). Embryo Development and Behavior in Sea
853 Urchin (*Tripneustes gratilla*) Under Different Light Emitting Diodes Condition. *Front. Mar. Sci.* 8: 684330
854 (2021). <https://doi.org/10.3389/fmars.2021.684330>
- 855 Mallefet J., Martinez-Soares P., Eléaume M., O'Hara T. and Duchatelet L. (2023). New insights on crinoid
856 (Echinodermata; Crinoidea) bioluminescence. *Front. Mar. Sci.* 10:1136138 (2023).
857 <https://doi.org/10.3389/fmars.2023.1136138>
- 858 Magnus, D. B. E. (1964) Gezeitenströmung und Nahrungsfiltration bei Ophiuren und Crinoiden.
859 *Helgoländer wiss. Meeresunters.* 10: 105-117.
- 860 Martínez-Morales J.R., Rodrigo I., and Bovolenta P. (2004). Eye development: a view from the retina
861 pigmented epithelium. *BioEssays : news and reviews in molecular, cellular and developmental biology.*
862 26(7):766-777 (2004). <https://doi.org/10.1002/bies.20064>
- 863 Mashanov V., Ademiluyi S., Jacob Machado D., Reid R. and Janies D. (2023) Echinoderm radial glia in
864 adult cell renewal, indeterminate growth, and regeneration. *Front. Neural Circuits* 17:1258370 (2023).
865 <https://doi.org/10.3389/fncir.2023.1258370>
- 866 Meyer D. L. (1973). Feeding Behavior and Ecology of Shallow-Water Unstalked Crinoids
867 (Echinodermata) in the Caribbean Sea. *Marine Biology* 22: 105-129 (1973).
868 <https://doi.org/10.1007/BF00391776>

- 869 Mironov A.N. and Pawson D.L. (2010). A new genus and species of Western Atlantic sea lily in the family
870 Septocrinidae (Echinodermata: Crinoidea: Bourgueticrinida). *Zootaxa* 2449: 49–68 (2010).
871 <https://doi.org/10.11646/zootaxa.2449.1.2>
- 872 Moore A. and Cobb J.L.S (1985) Neurophysiological studies on photic responses in *Ophiura ophiura*.
873 *Comparative Biochemistry and Physiology Part A: Physiology*. 80 (1): 11-16 (1985).
874 [https://doi.org/10.1016/0300-9629\(85\)90669-3](https://doi.org/10.1016/0300-9629(85)90669-3)
- 875 Oji T. and Twitchett R.J. (2015). The oldest post-Palaeozoic Crinoid and Permian-Triassic origins of the
876 Articulata (Echinodermata). *Zool Sci. Apr*;32(2):211-5 (2015). <https://doi.org/10.2108/zs140240>
- 877 Oliver Keller, Martin Kollmar, Mario Stanke, Stephan Waack (2011) A novel hybrid gene prediction
878 method employing protein multiple sequence alignments. *Bioinformatics*, 27(6): 757–763 (2011).
879 <https://doi.org/10.1093/bioinformatics/btr010>
- 880 Omori A., Shibata T.F. and Akasaka, K. (2020). Gene expression analysis of three homeobox genes
881 throughout early and late development of a feather star *Anneissia japonica*. *Dev Genes Evol* 230, 305–
882 314 (2020). <https://doi.org/10.1007/s00427-020-00665-6>
- 883 Parey E., Ortega-Martinez O., Delroisse J., Piovani L., Czarkwiani A., Dylus D., Arya S., Dupont S.,
884 Thorndyke M., Larsson T., Johannesson K., Buckley K., Martinez P., Oliveri P., and Marlétaz F. (2024).
885 The brittle star genome illuminates the genetic basis of animal appendage regeneration. *nature*
886 *ecology & evolution* (2024). <https://doi.org/10.1038/s41559-024-02456-y>
- 887 Petie, R., Hall, M. R., Hyldahl, M., & Garm, A. (2016). Visual orientation by the crown-of-thorns starfish
888 (*Acanthaster planci*). *Coral Reefs*, 35(4): 1139–1150 (2016). [https://doi.org/10.1007/s00338-016-](https://doi.org/10.1007/s00338-016-1478-0)
889 [1478-0](https://doi.org/10.1007/s00338-016-1478-0)
- 890 Ramirez M.D., Pairett A.N., Pankey M.S., Serb J.M., Speiser D.I., Swafford A.J., Oakley T.H. (2016). The
891 Last Common Ancestor of Most Bilaterian Animals Possessed at Least Nine Opsins. *Genome Biol. Evol.*
892 8(12): 3640–3652 (2016). <https://doi.org/10.1093/gbe/evw248>
- 893 Robinson J., Thorvaldsdóttir H., Turner D., Mesirov J. (2023). igv.js: an embeddable JavaScript
894 implementation of the Integrative Genomics Viewer (IGV). *Bioinformatics* 39(1), btac830 (2023).
895 <https://doi.org/10.1093/bioinformatics/btac830>
- 896 Roberts, A., Hill, N. A. and Hicks, R. (2000). Simple mechanisms organise orientation of escape
897 swimming in embryos and hatchling tadpoles of *Xenopus laevis*. *J. Exp. Biol.* 203, 1869–1885 (2000).
898 <https://doi.org/10.1242/jeb.203.12.1869>
- 899 Rouse GW, Jermiin LS, Wilson NG, Eeckhaut I, Lanterbecq D, Oji T, Young CM, Browning T, Cisternas P,
900 Helgen LE, Stuckey M, Messing CG. (2013). Fixed, free, and fixed: the fickle phylogeny of extant
901 Crinoidea (Echinodermata) and their Permian-Triassic origin. *Mol Phylogenet Evol.* 66(1):161-81
902 (2013). <https://doi.org/10.1016/j.ympev.2012.09.018>
- 903 Rutman J. and Fishelson L. (1969). Food composition and feeding behavior of shallow-water crinoids
904 at Eilat (Red Sea). *Mar. Biol.* 3: 46–57 (1969). <https://doi.org/10.1007/BF00355592>
- 905 Solovyev V, Kosarev P, Seledsov I, Vorobyev D. (2006) Automatic annotation of eukaryotic genes,
906 pseudogenes and promoters. *Genome Biol* 7 Suppl 1: S10. 1-12 (2006). [https://doi.org/10.1186/gb-](https://doi.org/10.1186/gb-2006-7-s1-s10)
907 [2006-7-s1-s10](https://doi.org/10.1186/gb-2006-7-s1-s10)
- 908 Stierwald M., Yanze N., Bamert R. P., Kammermeier L., and Schmid V. (2004). The *Sine oculis*/Six class
909 family of homeobox genes in jellyfish with and without eyes: Development and regeneration.
910 *Developmental Biology* 274: 70-81 (2004). <https://doi.org/10.1016/j.ydbio.2004.06.018>
- 911 Subha Kalyaanamoorthy, Bui Quang Minh, Thomas KF Wong, Arndt von Haeseler, and Lars S Jermiin
912 (2017). ModelFinder: Fast model selection for accurate phylogenetic estimates. *Nature Methods*,
913 14:587–589 (2017). <https://doi.org/10.1038/nmeth.4285>
- 914 Sumner-Rooney L., Rahman I.A., Sigwart J.D., Ullrich-Lüter E. (2018). Whole body photoreceptor
915 networks are independent of ‘lenses’ in brittle stars. *Proceedings of the Royal Society B: Biological*
916 *Sciences*, 285: 20172590 (2018). <https://doi.org/10.1098/rspb.2017.2590>

917 Sumner-Rooney L., Kirwan J.D., Lowe E., Ullrich-Lüter E. (2020). Extraocular Vision in a Brittle Star Is
918 Mediated by Chromatophore Movement in Response to Ambient Light. *Current Biology*, 30: 319–327
919 (2020). <https://doi.org/10.1016/j.cub.2019.11.042>
920 Sumner-Rooney L., Kirwan J.D., Lüter C. and Ullrich-Lüter E. (2021) Run and hide: visual performance
921 in a brittle star. *J. Exp. Biol.* 224 (11): jeb236653 (2021). <https://doi.org/10.1242/jeb.236653>
922 Sumner-Rooney L. & Ullrich-Lüter J. (2023). Extraocular vision in echinoderms. In *Distributed Vision:
923 From Simple Sensors to Sophisticated Combination Eyes* (pp. 49-85). Cham: Springer International
924 Publishing. https://doi.org/10.1007/978-3-031-23216-9_3
925 Takasu N. and Yoshida M. (1983). Photic effects on photosensory microvilli in the seastar *Asterias
926 amurensis*. *Zoomorphology* 103: 135-148 (1983). <https://doi.org/10.1007/BF00310473>
927 Terakita, A., Koyanagi, M., Tsukamoto, H. *et al.* Counterion displacement in the molecular evolution of
928 the rhodopsin family. *Nat Struct Mol Biol* 11, 284–289 (2004). <https://doi.org/10.1038/nsmb731>
929 Terakita A. The opsins. *Genome Biol* 6, 213 (2005). <https://doi.org/10.1186/gb-2005-6-3-213>
930 Terakita A., Kawano-Yamashita E., Koyanagi M. (2012). Evolution and diversity of opsins. *WIREs Membr
931 Transp Signal*, 1:104–111 (2012). <https://doi.org/10.1002/wmts.6>
932 Terakita A. and Nagata T. (2014). Functional Properties of Opsins and their Contribution to Light-
933 Sensing Physiology. *Zoological Science*, 31(10): 653-659 (2014). <https://doi.org/10.2108/zs140094>
934 Ullrich-Lüter E.M., Dupont S., Arboleda E., Hausen H., Arnone M.I. (2011). Unique system of
935 photoreceptors in sea urchin tube feet. *PNAS*, 108 (20): 8367–8372 (2011).
936 <https://doi.org/10.1073/pnas.1018495108>
937 Ullrich-Lüter E.M., D’Aniello S., Arnone M.I. (2013). C-opsin Expressing Photoreceptors in Echinoderms.
938 *Integrative and Comparative Biology*, 53 (1): 27–38 (2013). <https://doi.org/10.1093/icb/ict050>
939 Upton B., Díaz N., Gordon S., Van Gelder R., Buhr E., Lang R. (2021). Evolutionary Constraint on Visual
940 and Nonvisual Mammalian Opsins. *JOURNAL OF BIOLOGICAL RHYTHMS*, 36(2): 109–126 (2021).
941 <https://doi.org/10.1177/0748730421999870>
942 Vail L. (1987). Diel patterns of emergence of crinoids (Echinodermata) from within a reef at Lizard
943 Island, Great Barrier Reef, Australia. *Marine Biology* 93:551–560 (1987).
944 <https://doi.org/10.1007/BF00392793>
945 Varma N., Mutt E., Mühle J., Panneels V., Terakita A., Deupi X., Noglye P., Schertlera G., Lesca E. (2019).
946 Crystal structure of jumping spider rhodopsin-1 as a light sensitive GPCR. *PNAS*, 116(29): 14547-14556
947 (2019). <https://doi.org/10.1073/pnas.1902192116>
948 Wang M.H., Hsieh Y.J., Chang H.H., Wang Y. S. (2024). Effects of different visible light spectrums on
949 phototaxis and bottom preference behavior of sea cucumber. *Aquaculture* 578, 740112 (2024).
950 <https://doi.org/10.1016/j.aquaculture.2023.740112>
951 Weber W. and Grosmann M. (1977). Ultrastructure of the basiepithelial nerve plexus of the sea urchin,
952 *Centrostephanus longispinus*. *Cell Tissue Res.*, 175: 551–562 (1977).
953 <https://doi.org/10.1007/BF00222418>
954 Wintersinger J.A., Wasmuth J.D. (2014). Kablammo: an interactive, web-based blast results visualizer.
955 *Bioinformatics*, 31 (2014), pp. 1305-1306 (2014). <https://doi.org/10.1093/bioinformatics/btu808>
956 Yamamoto M., Yoshida M. (1978). Fine Structure of the Ocelli of a Synaptid Holothurian, *Opheodesoma
957 spectabilis*, and the Effects of Light and Darkness. *Zoomorphologie*, 90: 1 – 17 (1978).
958 <https://doi.org/10.1007/BF00993740>
959 Yoshida, M., Takasu, N., & Tamotsu, S. (1984). Photoreception in echinoderms. In *Photoreception and
960 vision in invertebrates* (pp. 743-771). Boston, MA: Springer US. [https://doi.org/10.1007/978-1-4613-
961 2743-1_22](https://doi.org/10.1007/978-1-4613-2743-1_22)
962 Zuber M.E., Gestri G., Viczian A.S., Barsacchi G. and Harris W.A. (2003). Specification of the vertebrate
963 eye by a network of eye field transcription factors. *Development*. 130(21): 5155-5167 (2003).
964 <https://doi.org/10.1242/dev.00723> Epub 2003 Aug 27. PMID: 12944429.

965

966 **Supplementary data:**

967 **Supplementary Table S1.** List of different opsin sequences from bilaterian species used for the *in silico*
968 and phylogenetic analysis.

969

970 **Supplementary Figure S1.** Phylogenetic analysis of Crinoid opsins. (A) Global phylogenetic tree of the
971 nine representative ancestral opsin lineages in bilaterian metazoans supported by maximum likelihood
972 method. Bootstrap values are indicated at the root of each opsin cluster and represented further in
973 the branch by a circle size proportional to the bootstrap value. Methodological details are presented
974 in the legend of Figure 4.

975

976 **Supplementary Figure S2.** Multiple alignment, identity and similarity values between the two
977 immunogenic peptides of the sea star (*Asterias rubens*) opsin 1.1 and opsin 4 recognised by antibodies
978 and the crinoid (*Antedon bifida*) opsin sequences. Other opsin sequences of the sea star *Asterias*
979 *rubens* and the sea urchin *Strongylocentrotus purpuratus* were added as model comparisons.

980

981 **Supplementary Figure S3.** Control tests for immunolabeling opsins in the ambulacral groove of the *A.*
982 *bifida* calyx: (A) immunofluorescence detection of opsin 4.1 in the basiepithelial nerve plexus (opsin
983 labelling in red and DAPI labelling of cell nuclei in blue). As sacculs are highly refractive structures,
984 they show strong red autofluorescence. (B) immunofluorescence detection of opsin 4.2 (in red) at the
985 tip of tube feet. (C) Immunohistochemistry detection of opsin 4.2 (in brown) at the tip of tube feet. (D)
986 Negative control in immunofluorescence without antibodies. (E) Negative control in
987 immunofluorescence with rabbit preimmune serum. (F) Negative control in immunohistochemistry
988 without antibodies.